NASA CR-759

ELECTRON SCATTERING AND BREMSSTRAHLUNG CROSS-SECTION MEASUREMENTS

By D. H. Rester and W. E. Dance

Prepared under Contract No. NASw-1385 by
LING-TEMCO-VOUGHT, INC.
Dallas, Texas

for

NATIONAL AERONAUTICS AND SPACE ADMINISTRATION

For sale by the Clearinghouse for Federal Scientific and Technical Information
Springfield, Virginia 22151 – CFSTI price $3.00

TABLE OF CONTENTS

TABLE OF CONTENTS

LIST OF FIGURES

ELECTRON SCATTERING

Introduction

Measurements of the cross sections for Coulomb scattering of electrons without atomic excitation by Al and of the electron penetration spectra due to bombardment of thick Al slabs were previously reported and published in NASA Contractor Report NASA CR-334.[1] The present report contains the results of additional thick target transmission measurements on Al, thick target transmission measurements on Au, and electron backscattering measurements on targets of Al, Fe, Sn, and Au. Where the data is available comparisons are made to the Monte Carlo calculations of M. J. Berger.

Experimental Results

Electron Transmission Spectra

Aluminum. The initial measurements of electron transmission spectra for the case of 1-MeV electrons with normal incidence on Al slabs were generally in good agreement with the Monte Carlo calculations of M. J. Berger. Measurements were reported for thicknesses corresponding to 0.2, 0.4, and 0.6 the range of 1-MeV electrons in Al (0.11 g/cm^2, 0.22 g/cm^2, and 0.33 g/cm^2 respectively). Comparisons of energy spectra normalized with respect to the incident number of electrons and the solid angle increment were made at various angles in the forward half of the sphere. This type of comparison was considered to be the most meaningful and detailed that could be made in terms of "testing" the calculations. At the time of the previous report only a limited number of spectra had been measured for the penetration of the 0.33-g/cm^2 slab. In addition the data for the 0.11-g/cm^2 slab, where the penetration is greatest, was assigned an uncertainty of 20%, or twice the uncertainty assigned to the measurements at the other thicknesses. Thus to complete the transmission measurements for Al additional spectra for the 0.33-g/cm^2 thickness were accumulated so that the energy spectra for all three thicknesses could be integrated over solid angle to obtain total transmission spectra, and additional measurements were made for

the 0.11-g/cm^2 slab to reduce the experimental error. The integrated spectra for the three slab thicknesses are shown in Figs. 1-3 compared with two different Monte Carlo calculations of Berger, labeled Set A and Set B, and the transmitted fraction, in Fig. 4. The details of these calculations have not been made available in published form. As can be seen the agreement between the calculations and the experiment for the thickest slab is quite good. The agreement is not quite as good for the intermediate thickness, where the calculated spectrum begins to sharpen relative to the experimental spectrum, and for the thinnest layer, where the discrepancy appears to be in both shape and area, or yield. Remeasurement of the penetration spectra has yielded a result indicating that the measured transmission yield shown in Fig. 1 should be reduced by less than 5%, so that there still appears to be a discrepancy for this thickness which, while it is well within the limits suggested by the combined uncertainties of the experiment and calculation, is still greater than the differences for the other two thicknesses. Comparisons of the calculated and measured angular distributions are shown in Fig. 5. This figure is similar to the angular distributions of Report NASA CR-334 except that additional points are included for the 0.33-g/cm^2 thickness and that the re-measured yields at angles less than 30 deg for the 0.11-g/cm^2 thickness are on the average 10% lower than the previously reported values.

The experimental arrangement and the experimental techniques employed to carry out the measurements and to reduce the energy spectra are identical with those used previously and described fully in NASA CR-334. However, the measurements for the 0.11-g/cm^2 thickness at the most forward angles present a special problem since here the counting rates for measurable beam intensities saturate the counting system. To overcome this problem, which had led to the large uncertainties in the previous data, ordinary beam current integration was abandoned and a beam monitor was used. The monitor was a solid state detector positioned at 135 deg which counted back-directed electrons while the measurements were made at the forward angles. The yield of backscattered electrons at 135 deg was much less than those penetrating the slab in nearly the straight-through direction and could be easily related to the beam current.

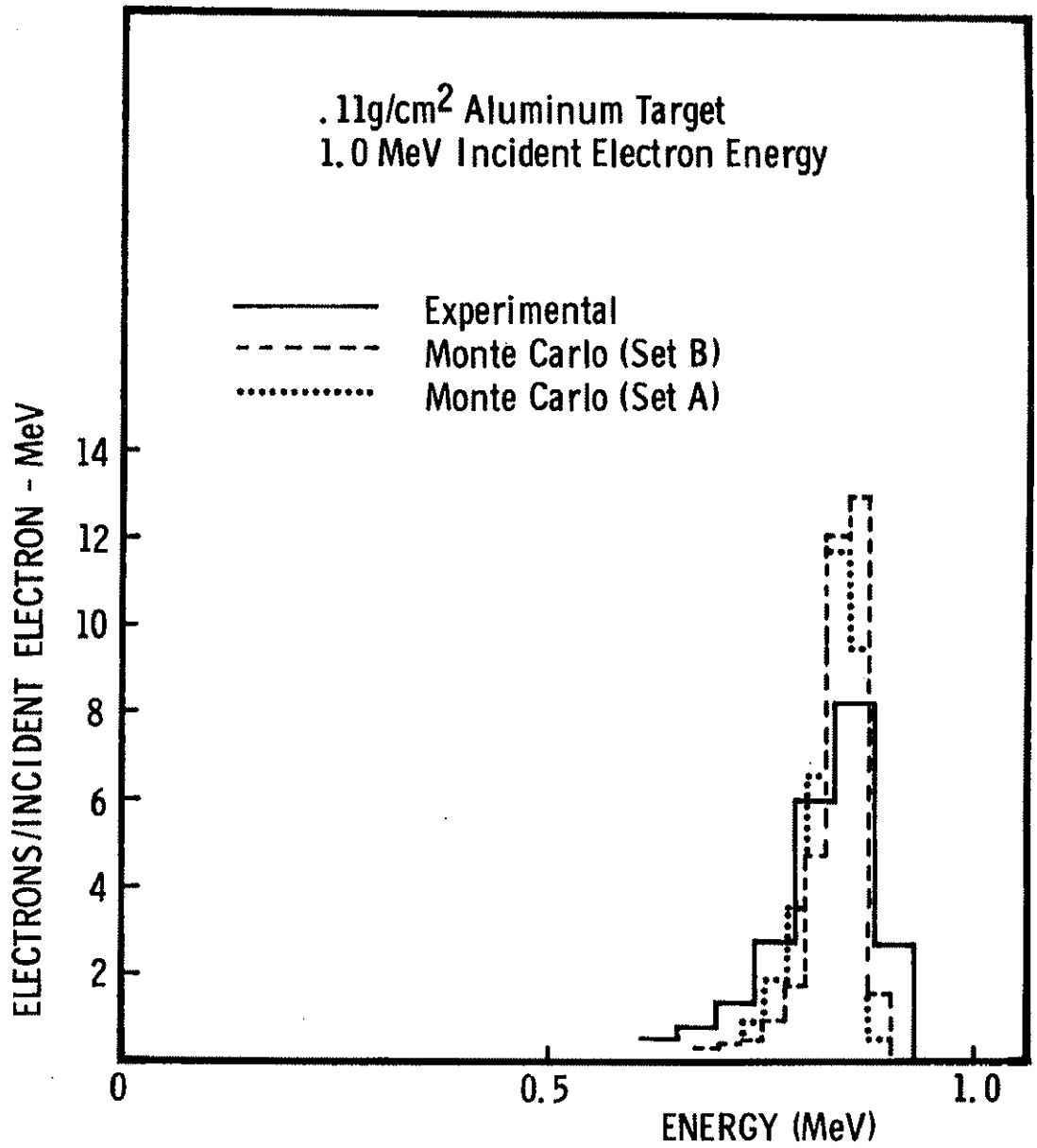

Figure 1. Total energy spectrum of transmitted electrons for 0.11-g/cm^2 Al slab.

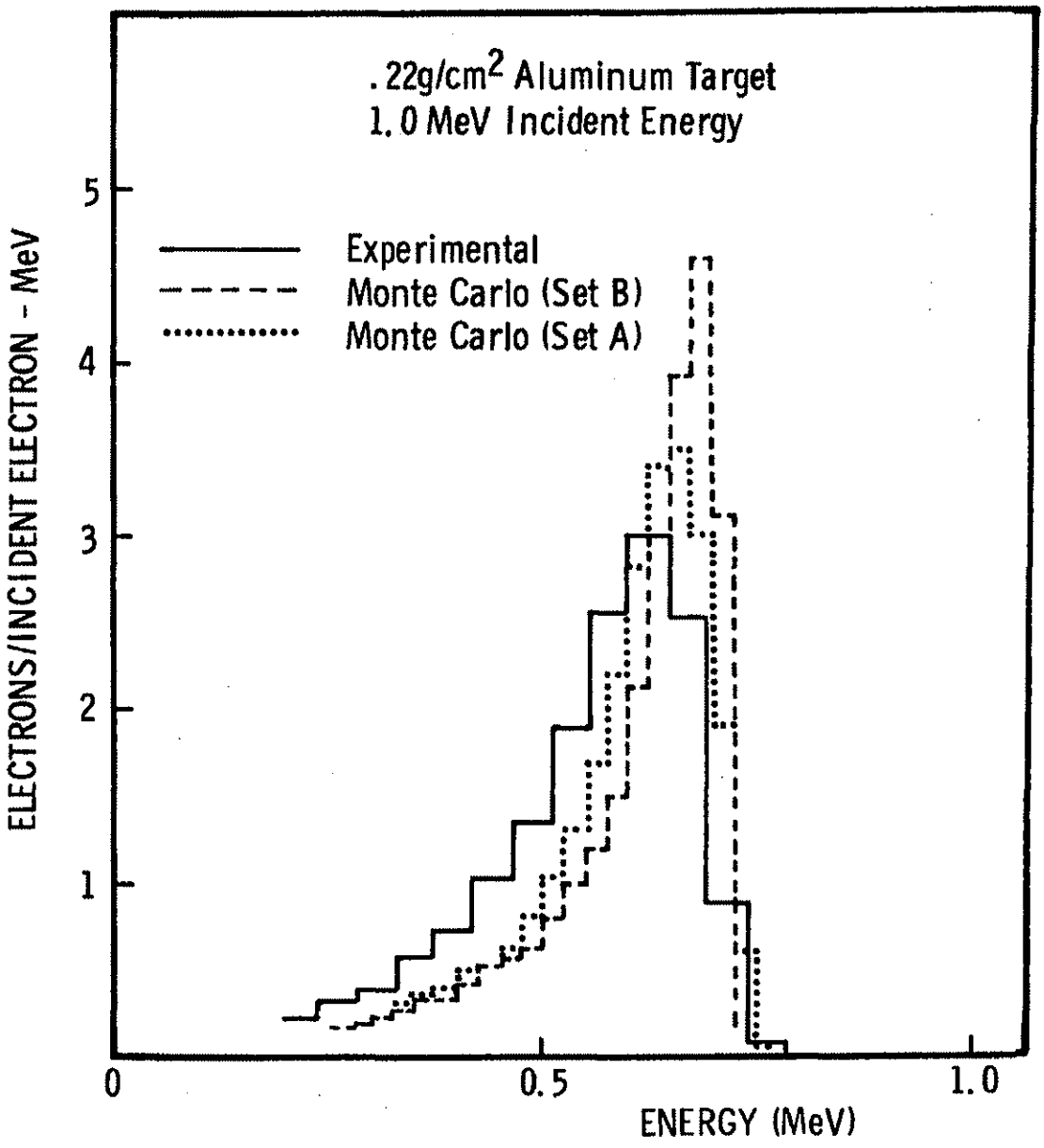

Figure 2. Total energy spectrum of transmitted electrons for 0.22-g/cm^2 Al slab.

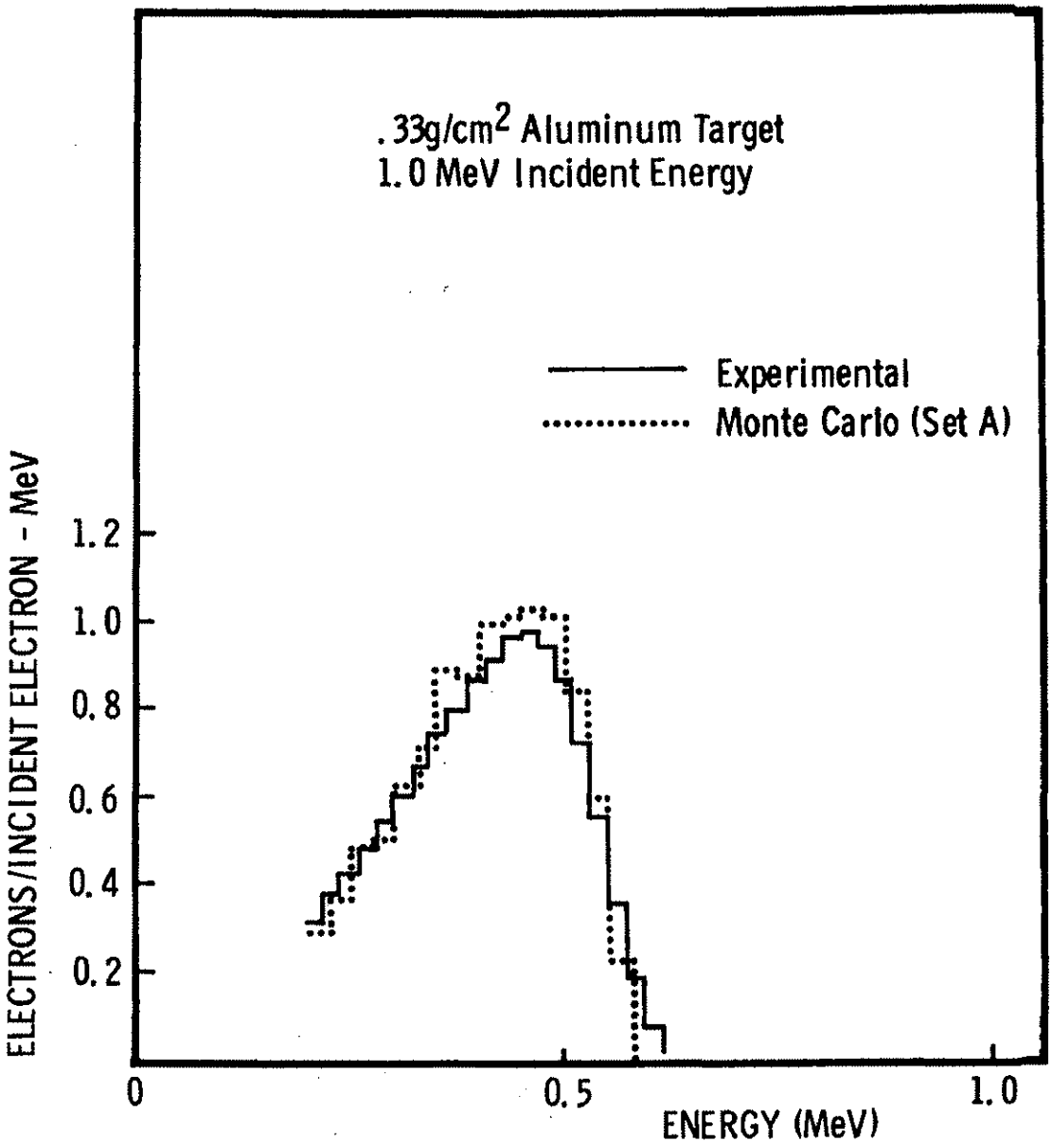

Figure 3. Total energy spectrum of transmitted electrons for 0.33-g/cm^2 Al slab.

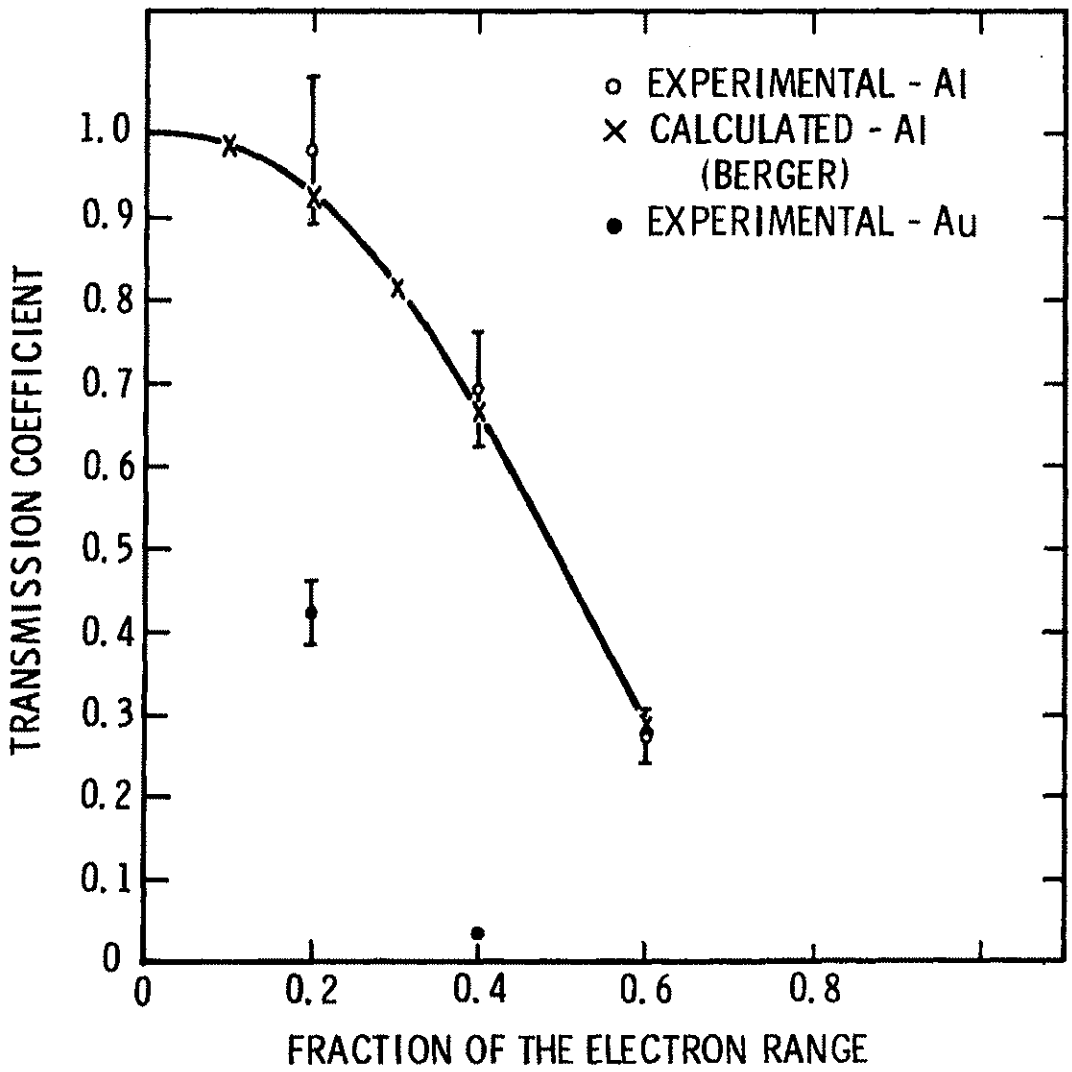

Figure 4. Transmitted fraction of 1-MeV electrons with normal incidence on various thicknesses of Al and Au as a function of thickness.

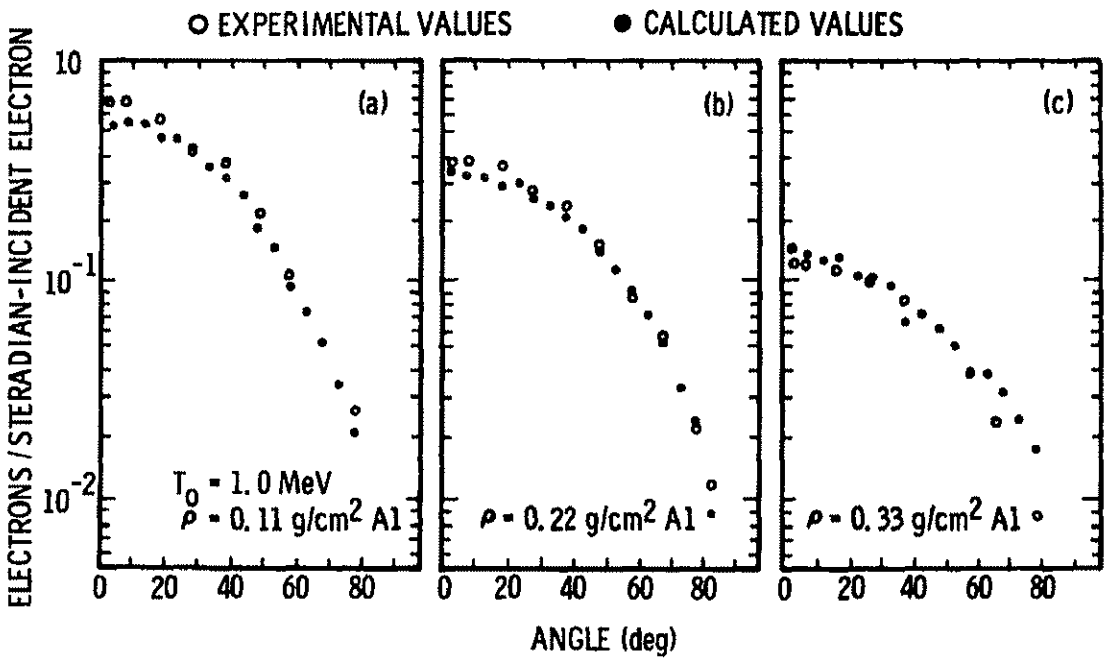

Figure 5. Angular distributions of transmitted electrons for 0.11-, 0.22-, and 0.33-g/cm^2 Al slabs.

The final experimental values reported are believed to be not more than 10% from the true values.

Gold. The transmission spectra for 1-Mev electrons with normal incidence on slabs of Au corresponding to thicknesses of 0.192 and 0.405 the range of 1-MeV electrons in Au are shown at three angles for each thickness in Figs. 6 and 7. Distributions at 2.5, 37.5 and 77.5 deg illustrate the fact that the spectra are nearly constant with angle for a given thickness. The angular distributions of transmitted electrons are shown in Fig. 8 and the energy spectra integrated over solid angle are shown in Fig. 9. A comparison of the transmission spectra for the same fraction of the range in both Al and Au is shown in Fig. 10. The transmitted beam fractions corresponding to these spectra are presented in Fig. 4. These measurements were carried out in the same manner as that described for the Al slabs. However, due to the relatively lower transmission of the Au slabs and the increased bremsstrahlung production efficiency of Au, bremsstrahlung backgrounds became a more significant problem for these measurements. This is illustrated in Fig. 11 which shows the relative intensity of the bremsstrahlung to the total yield for $\theta = 77.5$ deg for each thickness. These spectra represent the cases where the background is largest. Even so, it can be removed accurately from the data and does not have a serious effect on the accuracy of the net spectra.

The experimental uncertainty in the measurement of Au transmission spectra is about 7% and arises as for the case of Al primarily from the determination of the number of incident electrons.

Electron Backscatter Spectra

The energy spectra at various angles due to backscattering from target materials of several different atomic numbers are shown in Figs. 12-15. In all cases the incident electron beam was directed with normal incidence to the target and the beam energy was fixed at 1 MeV. Target materials of Al (Z=13), Fe (Z=26), Sn (Z=50), and Au (Z=79) were used in the experiment. This allowed a systematic study of the dependence of the spectral distributions and the total backscatter fraction on atomic

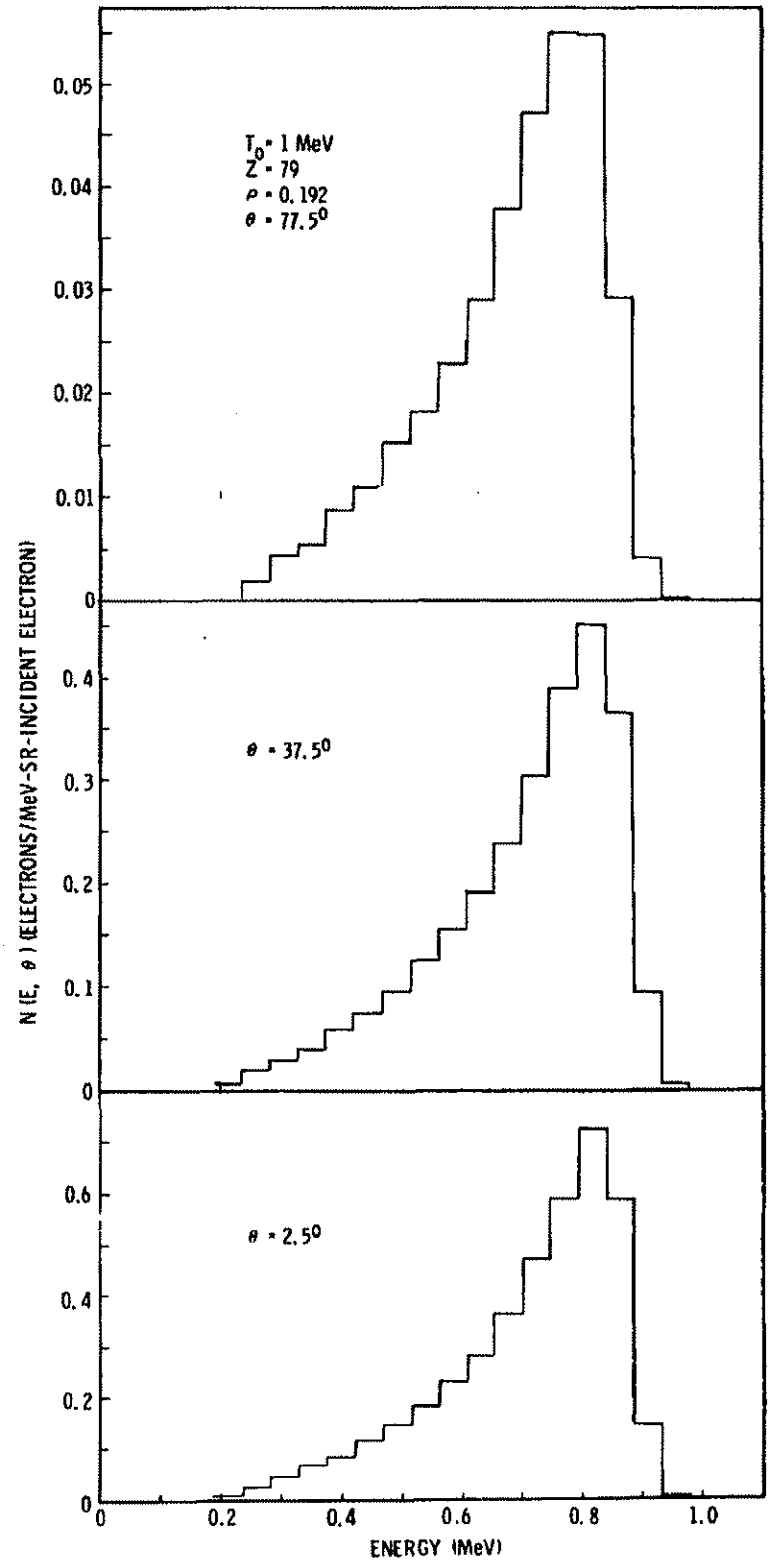

Figure 6. Energy spectra of transmitted electrons for a 0.14-g/cm^2 Au slab at θ = 2.5, 37.5, and 77.5 deg.

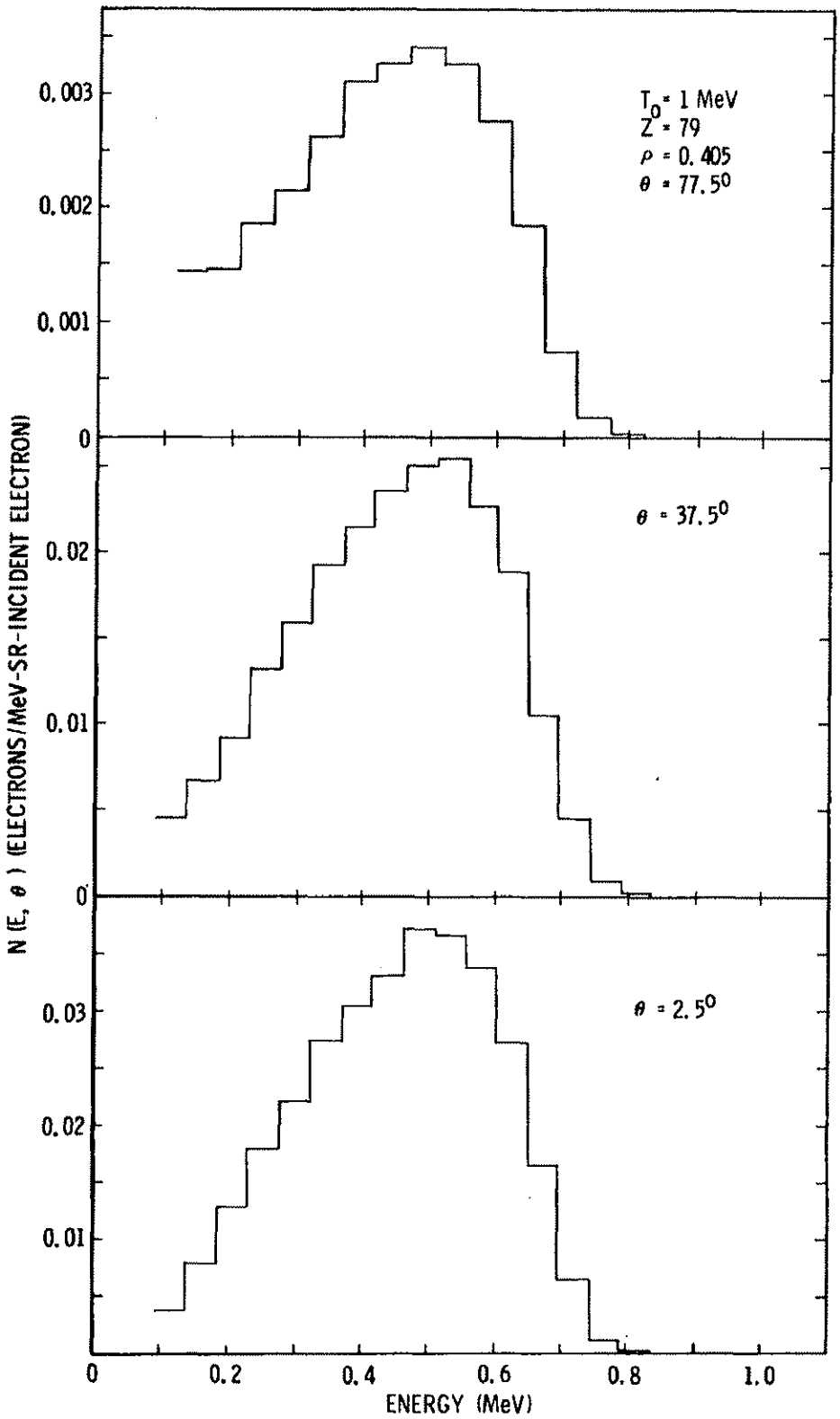

Figure 7. Energy spectra of transmitted electrons for a 0.30-g/cm^2 Au slab at θ = 2.5, 37.5, and 77.5 deg.

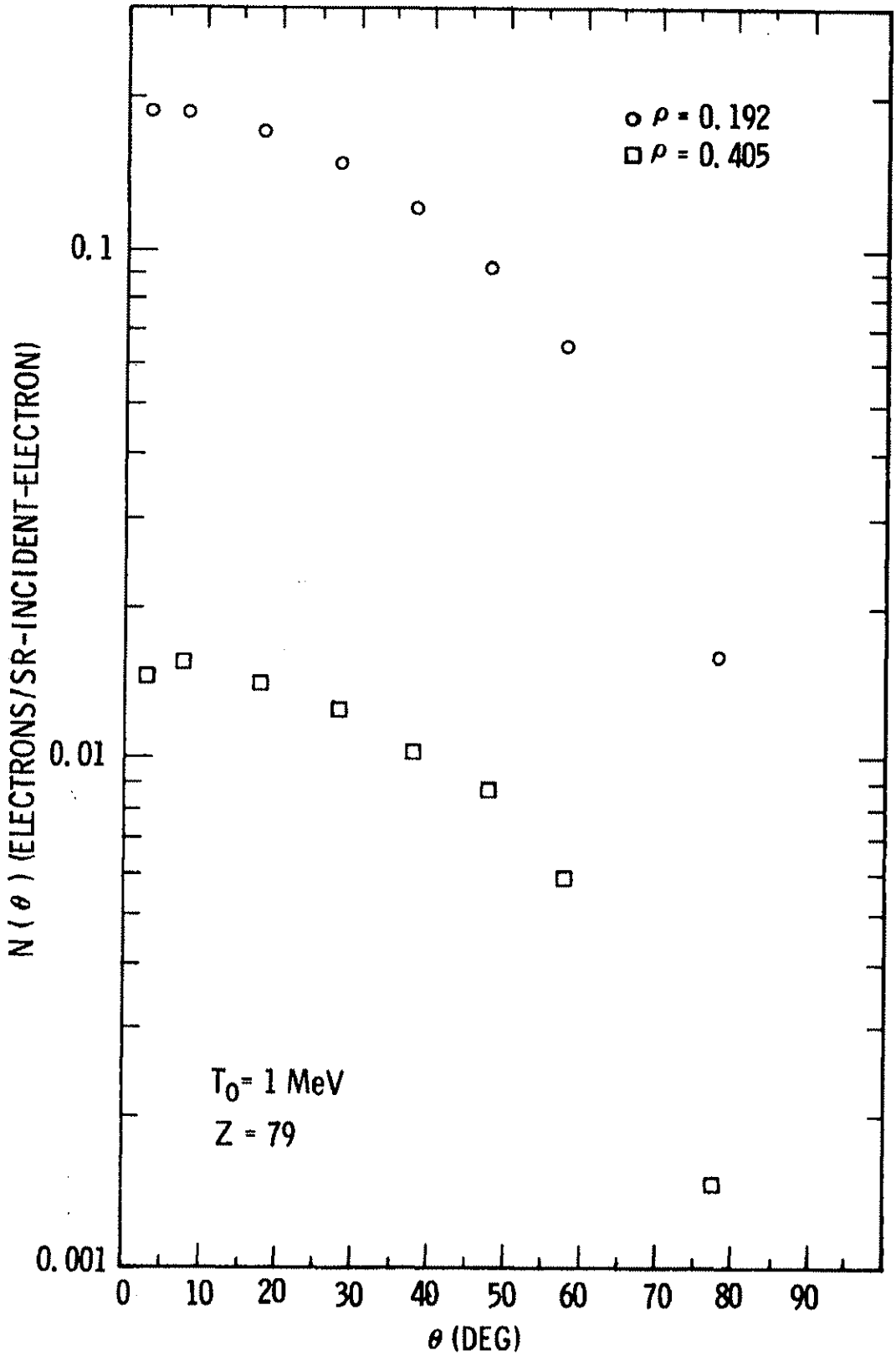

Figure 8. Angular distributions of transmitted electrons for 0.14- and 0.30-g/cm^2 Au slabs.

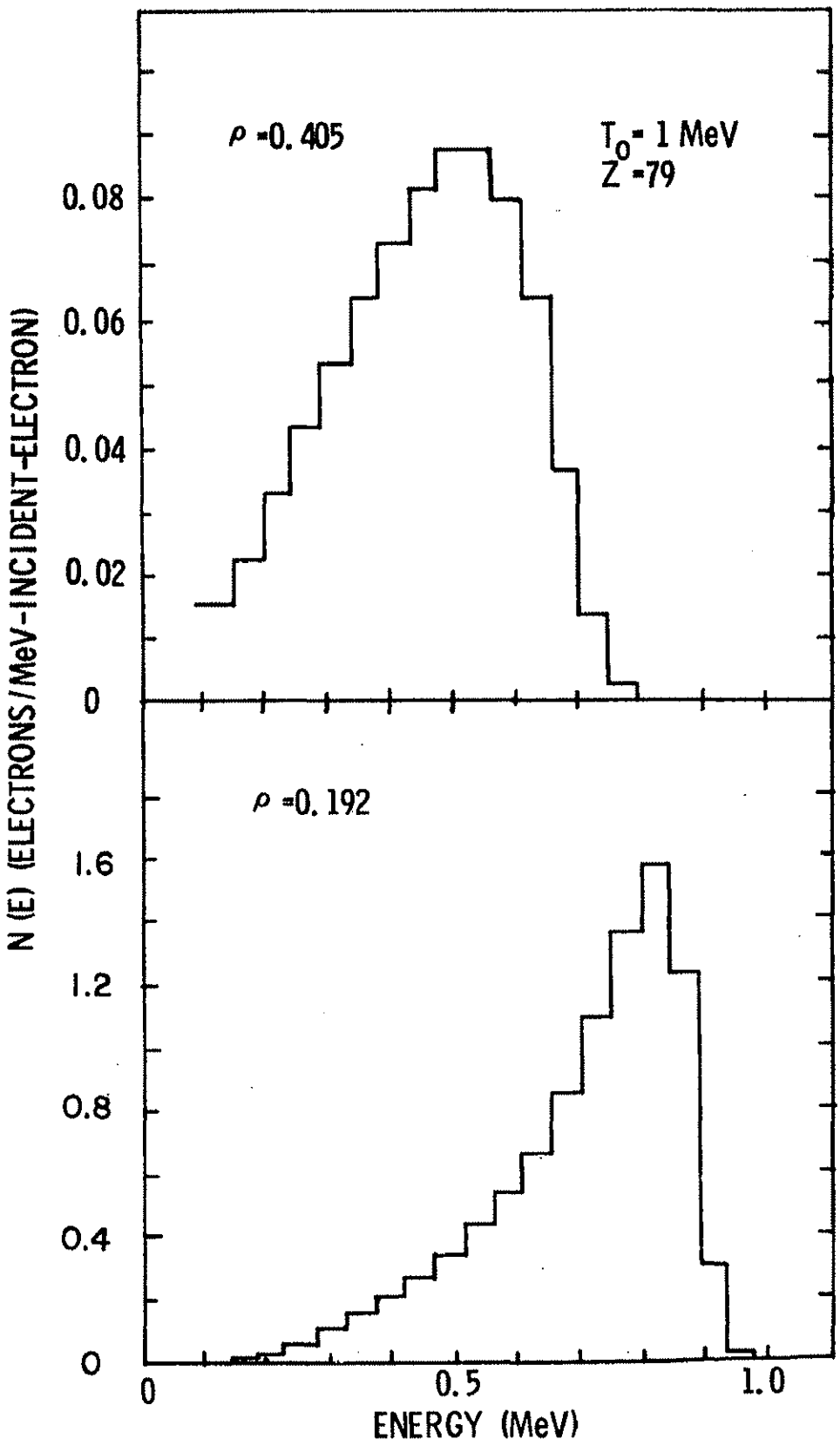

Figure 9. Total energy spectra of transmitted electrons for 0.14-g/cm^2 and 0.30-g/cm^2 Au slabs.

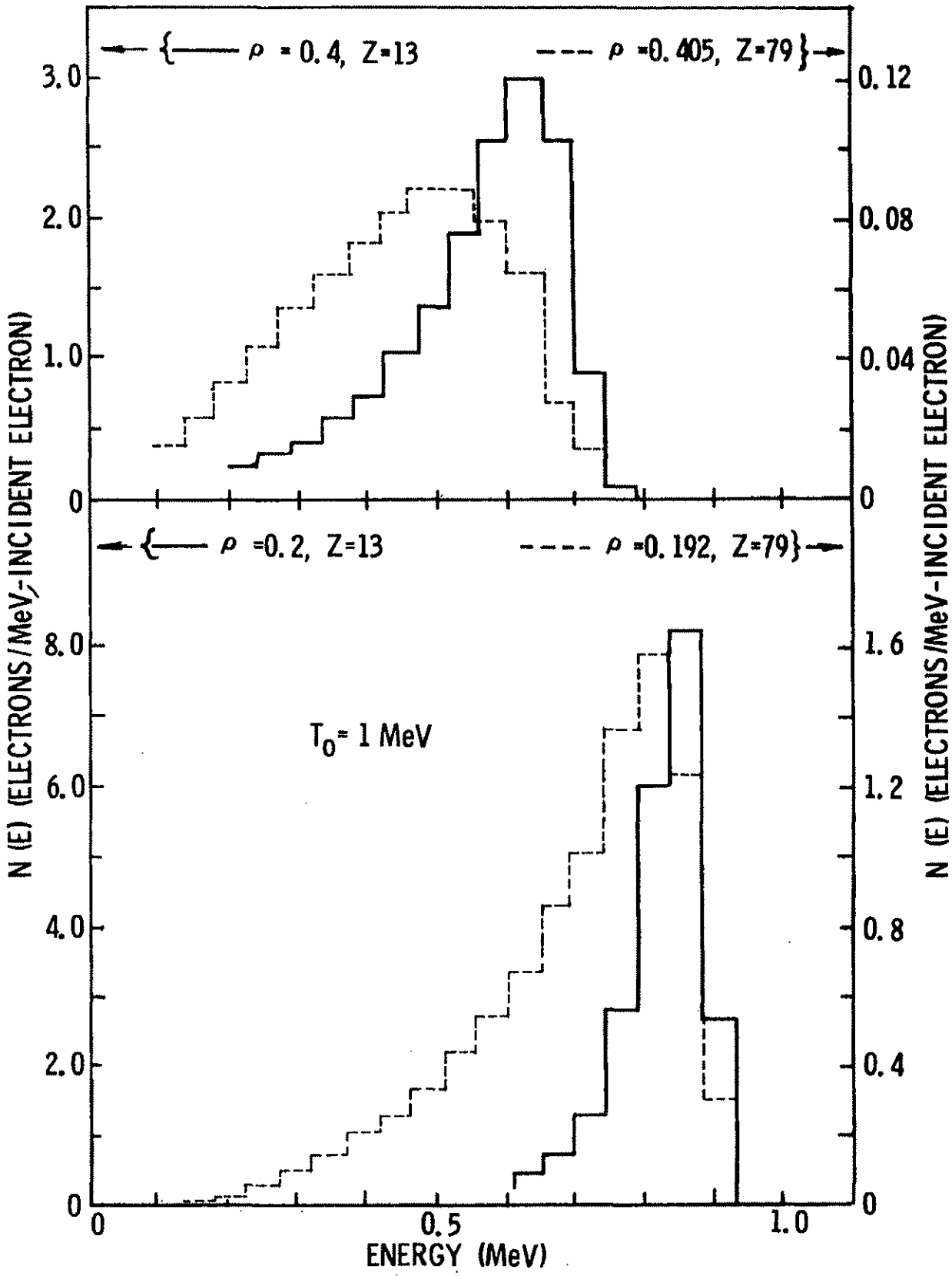

Figure 10. Comparisons of total energy spectra of transmitted electrons for thicknesses corresponding to the same fractions of the range for Al and Au.

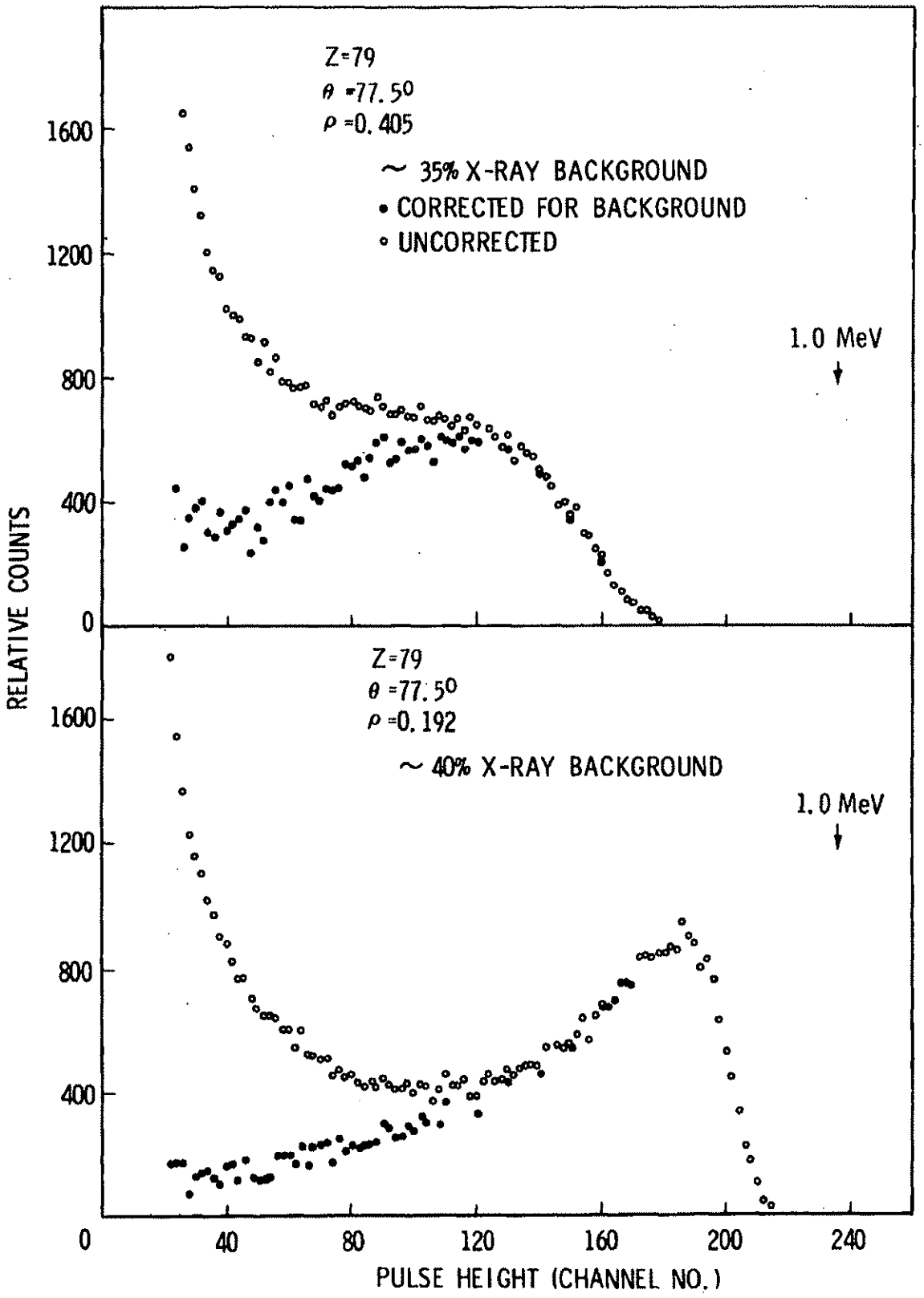

Figure 11. Examples of pulse height distributions showing the x-ray backgrounds and their removal to obtain the net electron distributions.

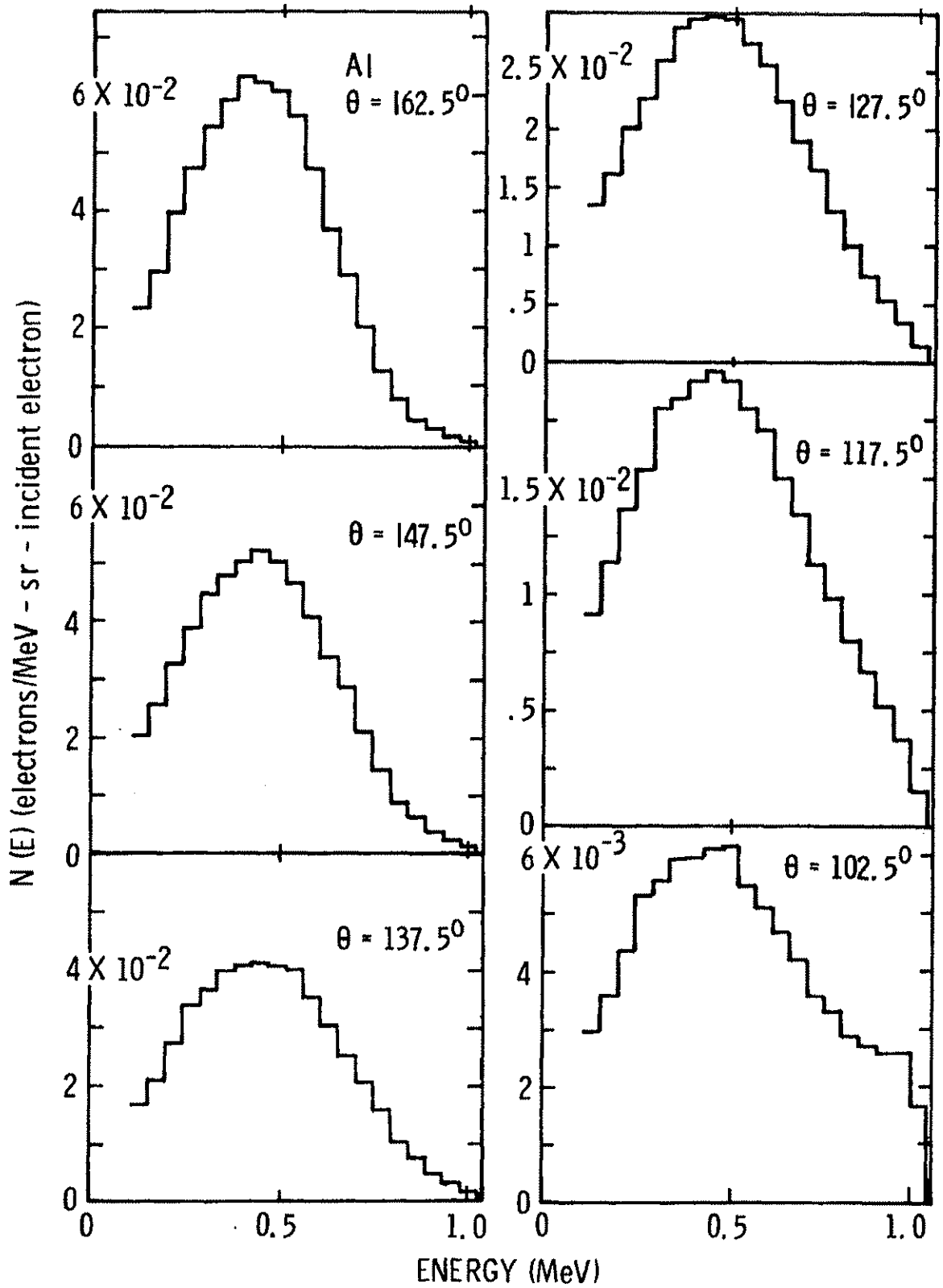

Figure 12. Backscattered-electron energy spectra due to 1-MeV electrons with normal incidence on a saturation thickness of Al.

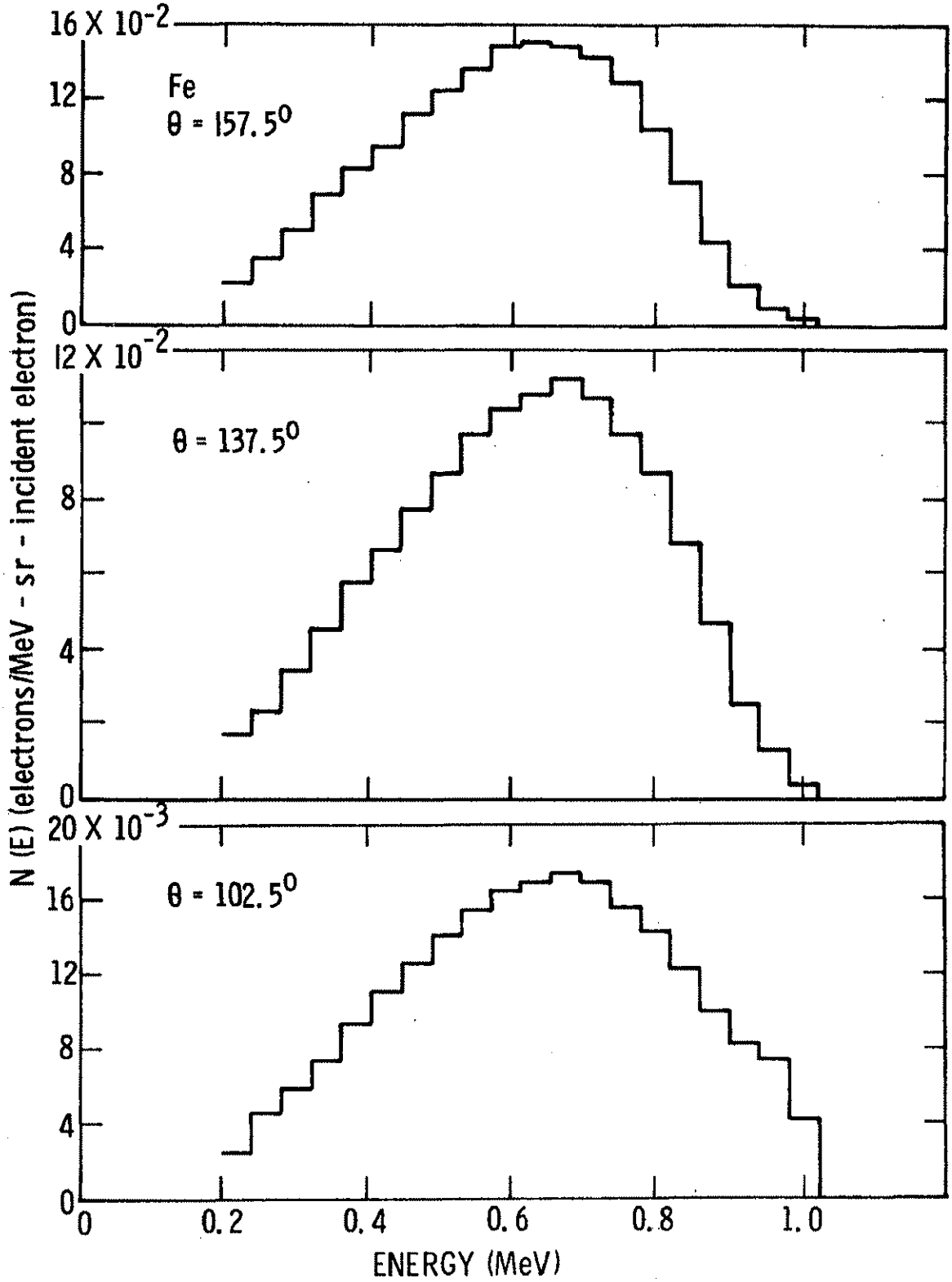

Figure 13. Backscattered-electron energy spectra due to 1-MeV electrons with normal incidence on a saturation thickness of Fe.

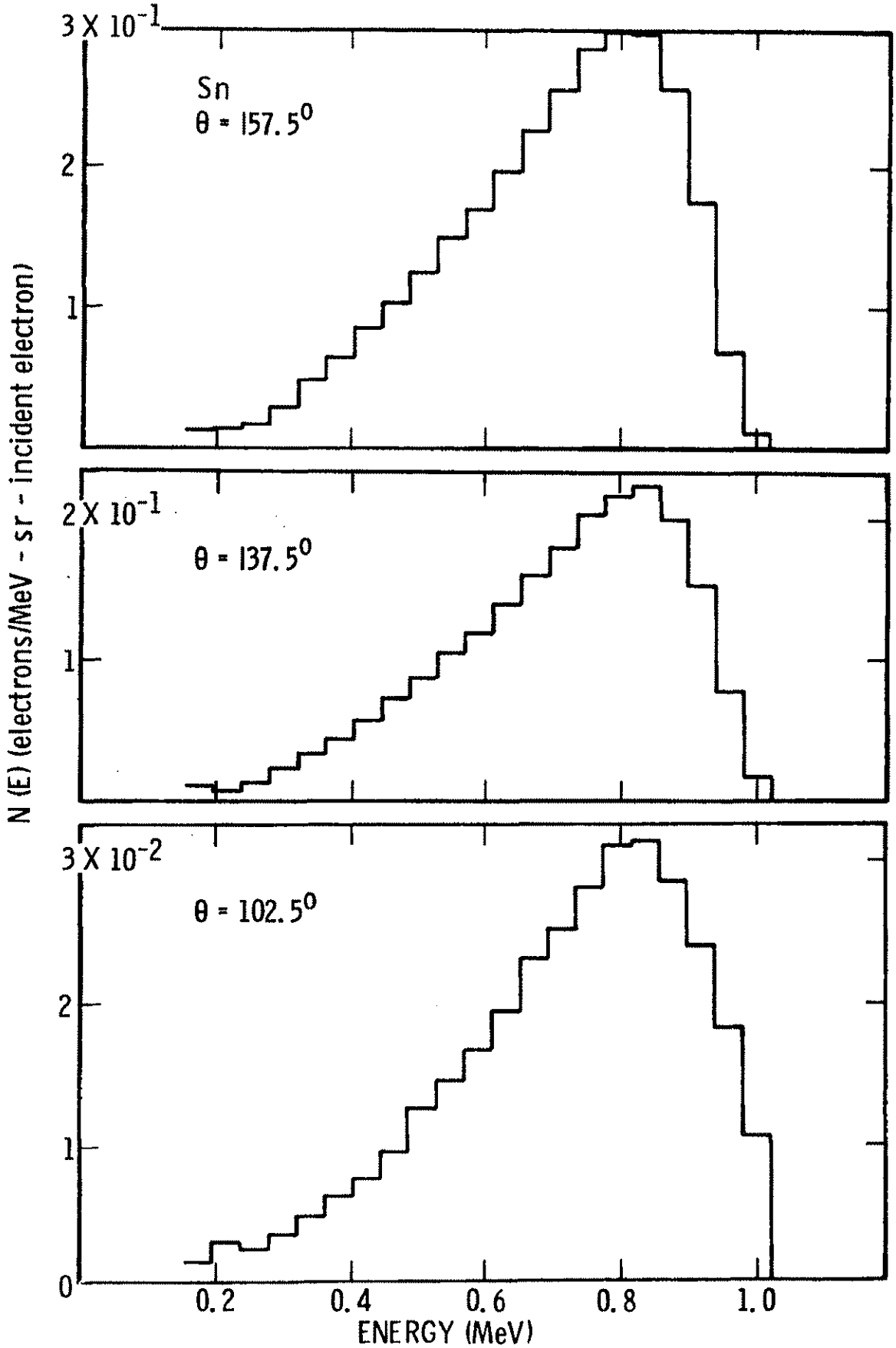

Figure 14. Backscattered-electron energy spectra due to 1-MeV electrons with normal incidence on a saturation thickness of Sn.

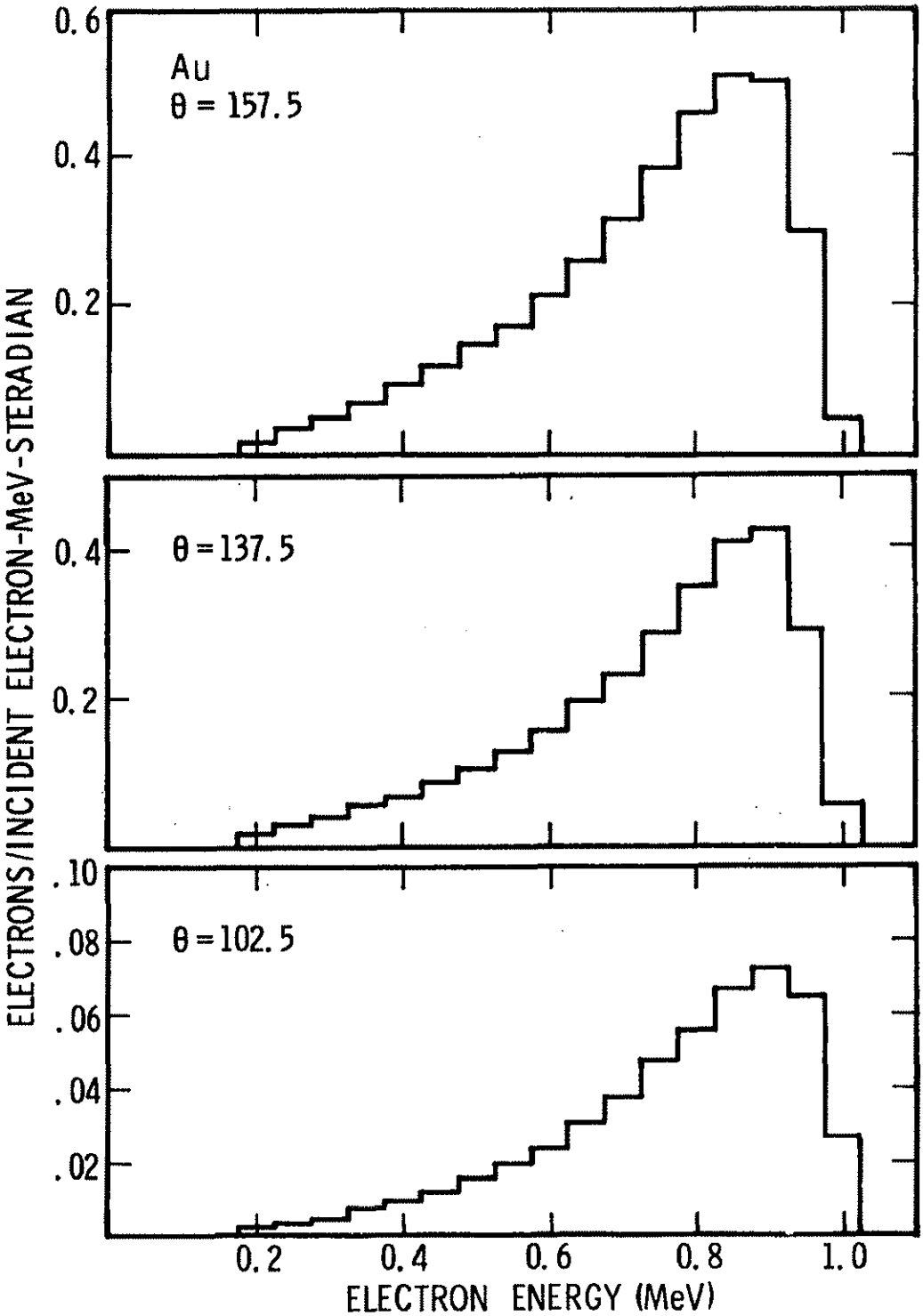

Figure 15. Backscattered-electron energy spectra due to 1-MeV electrons with normal incidence on a saturation thickness of Au.

number to be made. Measurements were made on saturation thicknesses of the target materials for backscattering, which amounted to a thickness corresponding to 0.4 the range of 1-MeV electrons for each material in the present case. The angular distributions of backscattered electrons are shown in Fig. 16. Figure 17 shows the backscattered energy distributions integrated over solid angle. Also shown in the figure is the spectrum of backscattered electrons from a thickness of Al corresponding to less than a saturation thickness, namely a thickness of 0.22 g/cm^2. Figure 18 shows the backscatter fraction of the present experiment in the energy region above 0.1 MeV corrected by about 3% due to yield below 0.1 MeV as estimated by extrapolation of the data below this energy. The backscatter fraction is plotted versus atomic number, along with a similar set of backscatter fractions measured by Wright and Trump[2] by a different technique. The limit of error assigned to the present experiment is 7%. The differences obtained by the two methods are outside the estimated experimental error. Discrepancies of this order have been seen in other measurements where both of these techniques have been employed. However, the present method is as accurate for backscatter measurements as for penetration measurements where good agreement with the calculations have been obtained. Also the present backscatter fractions are in agreement with the backscatter fraction observed from CsI crystal scintillation spectrometers where a direct measurement of backscatter can be made.

Several interesting features of backscattering due to normal incidence are apparent from the backscattering data. The most probable energy of the backscatter distribution increases with atomic number. The total backscatter spectra for the lower Z materials not only have a lower most probable energy than those for higher Z materials but also are considerably broader. In the case of Al and Fe at angles of observation near the target plane a high energy shelf develops in the distributions due to a relatively large contribution from scattering at the surface of the slab as compared to the contribution from greater depths. The spectrum from the 0.22-g/cm^2 slab of Al shown in Fig. 17 plotted over the spectrum from the saturation thickness of Al allows an identification of the contributions from the different thicknesses to be made. Finally, the total backscatter coefficient increases with atomic number.

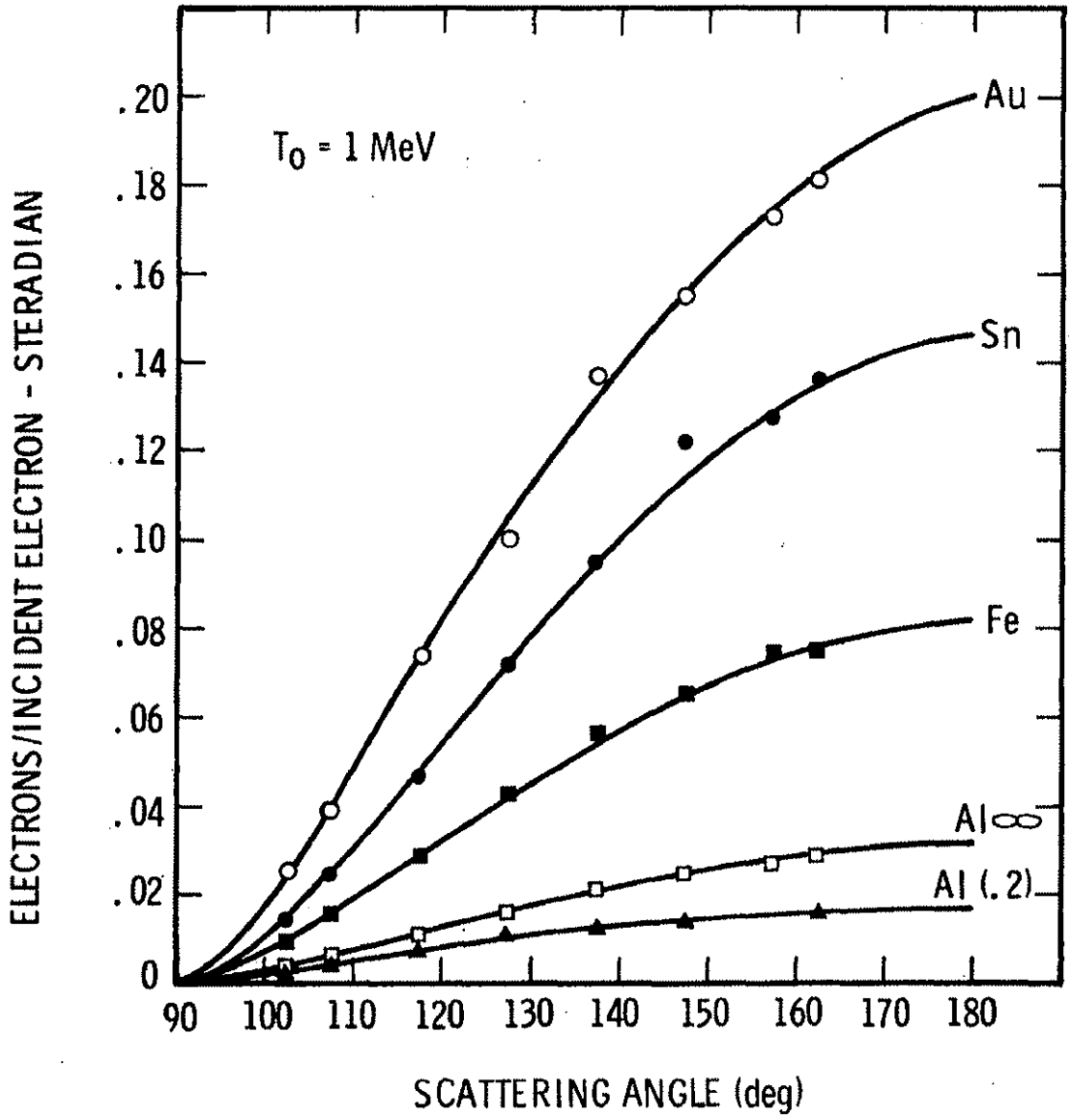

Figure 16. Angular distributions of backscattered electrons.

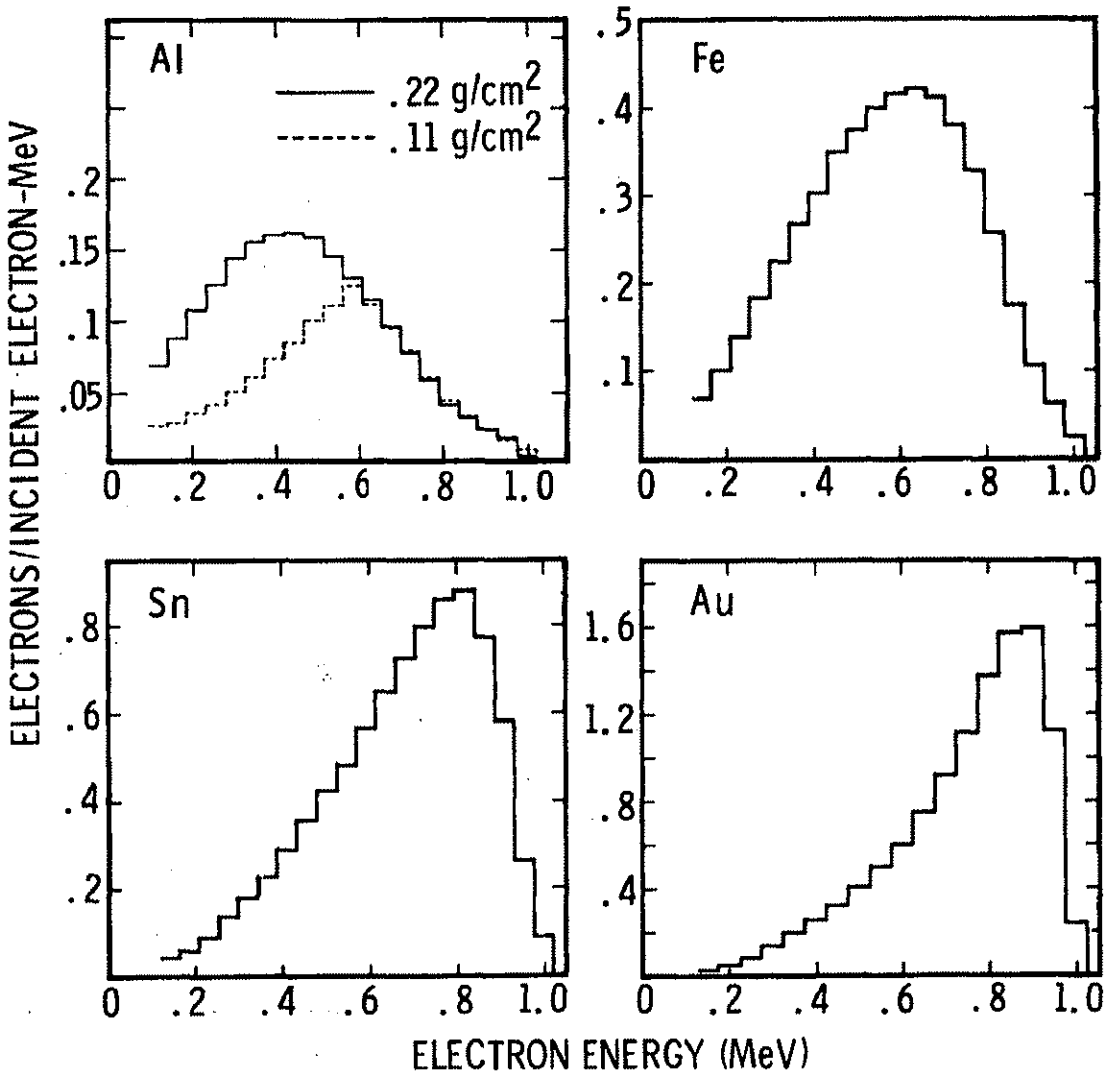

Figure 17. Total energy distributions of backscattered electrons for incident 1-MeV electrons with normal incidence.

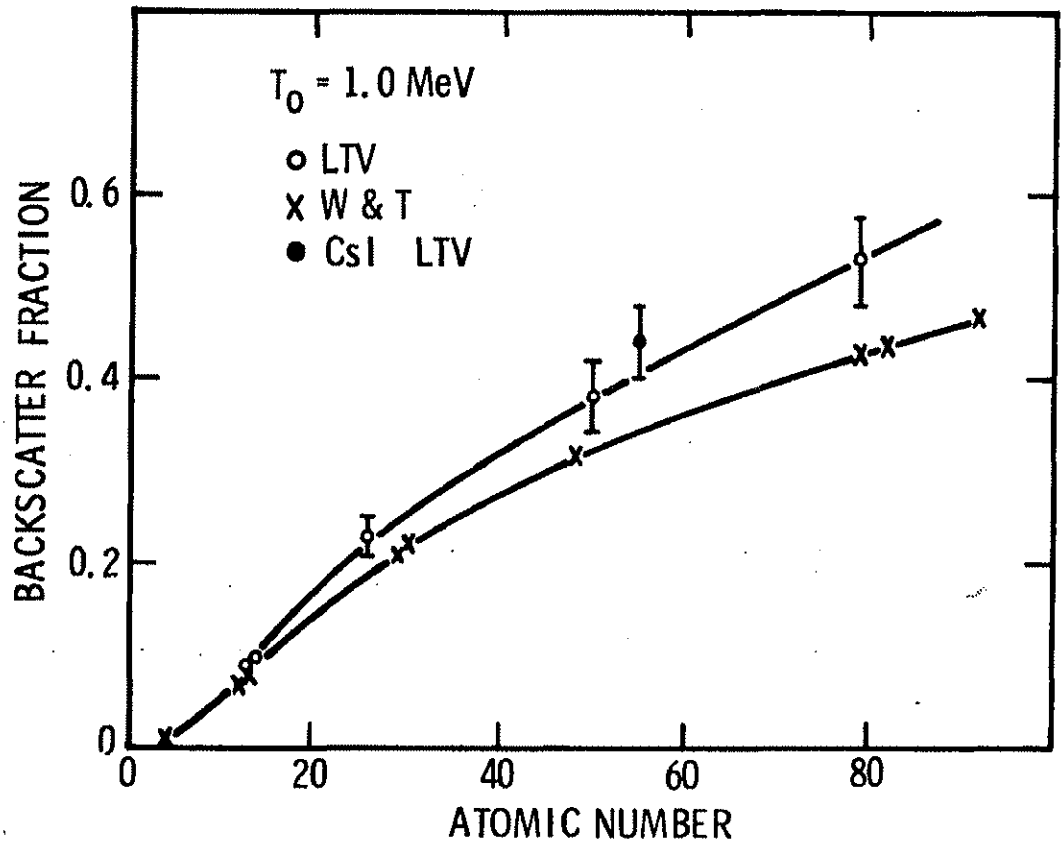

Figure 18. Backscattered fraction for 1-MeV electrons with normal incidence on slabs of saturation thicknesses as a function of atomic number.

ELECTRON-BREMSSTRAHLUNG CROSS SECTION MEASUREMENTS

Introduction

Measurements of electron-bremsstrahlung cross sections for Al, Cu, Sn, and Au have been completed for an incident electron energy T_o = 1.0 MeV. Cross sections for Al have been completed for the additional electron energies T_o = 1.7 and 2.5 MeV. The experimental values are shown graphically with the Bethe-Heitler values for an unscreened nucleus to allow an easy comparison of the experimental results to the theory. Tables of experimental values are also included so that the values may be obtained accurately for comparison to other calculations such as those now being carried out by C. D. Zerby[3] of the Union Carbide Research Institute. Although the results presented are in some instances only first measurements, the cross sections are believed to be free from unknown experimental errors. Measurements to confirm the data presented here will be made in the near future. At the same time data for Cu, Sn, and Au at T_o = 1.7 and 2.5 MeV will be obtained. Results of these experiments will be made available in the quarterly reports as they become available. Previous results of cross-section measurements at θ=15 and 30 deg for T_o = 0.5 and 1.0 MeV and Z=13 were given in NASA Contractor Report NASA CR-334. Since the earlier data was preliminary data only, it should be considered as being replaced by the present results.

Experimental Results and Procedure

The experimental cross sections for bremsstrahlung production by 1-MeV electrons scattered by Al, Cu, Sn, and Au atoms compared to the Sauter cross sections[4] (plane-wave Born approximation, unscreened) are shown in Figs. 19-23. Comparisons at 1.7 and 2.5 MeV for Al are shown in Figs. 24 and 25. Tables I and II contain the cross-section values plotted in the figures. Table I includes values over the complete spectral range above about $k = 0.1\ T_o$. Table II includes values from about $k \approx 0.6\ T_o$ to the end points. The values in Table II have been used in the figures instead of their counterparts in Table I because of their improved accuracy. The experimental results are in good agreement with the

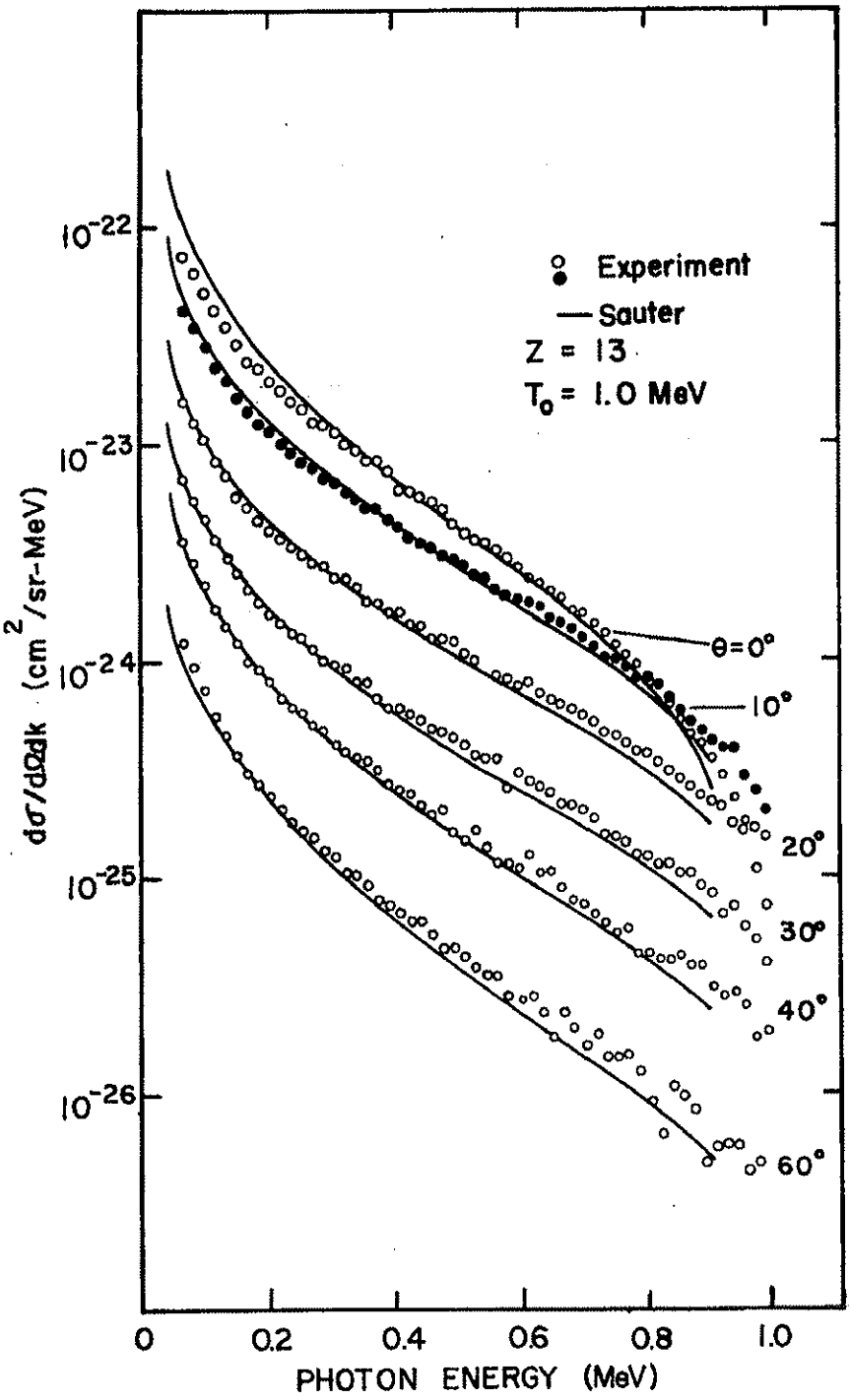

Figure 19. Bremsstrahlung differential cross sections for 1.0-MeV electrons on Al.

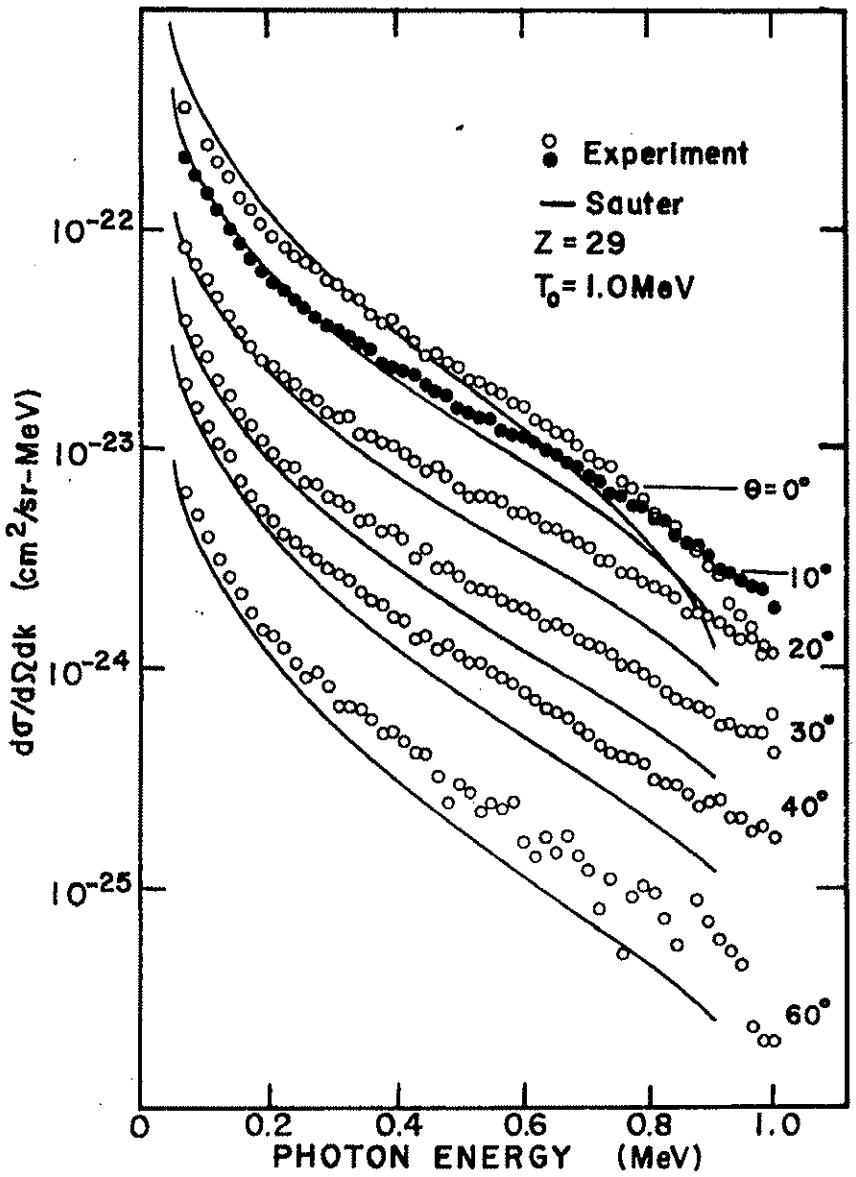

Figure 20. Bremsstrahlung differential cross sections for 1.0-MeV electrons on Cu.

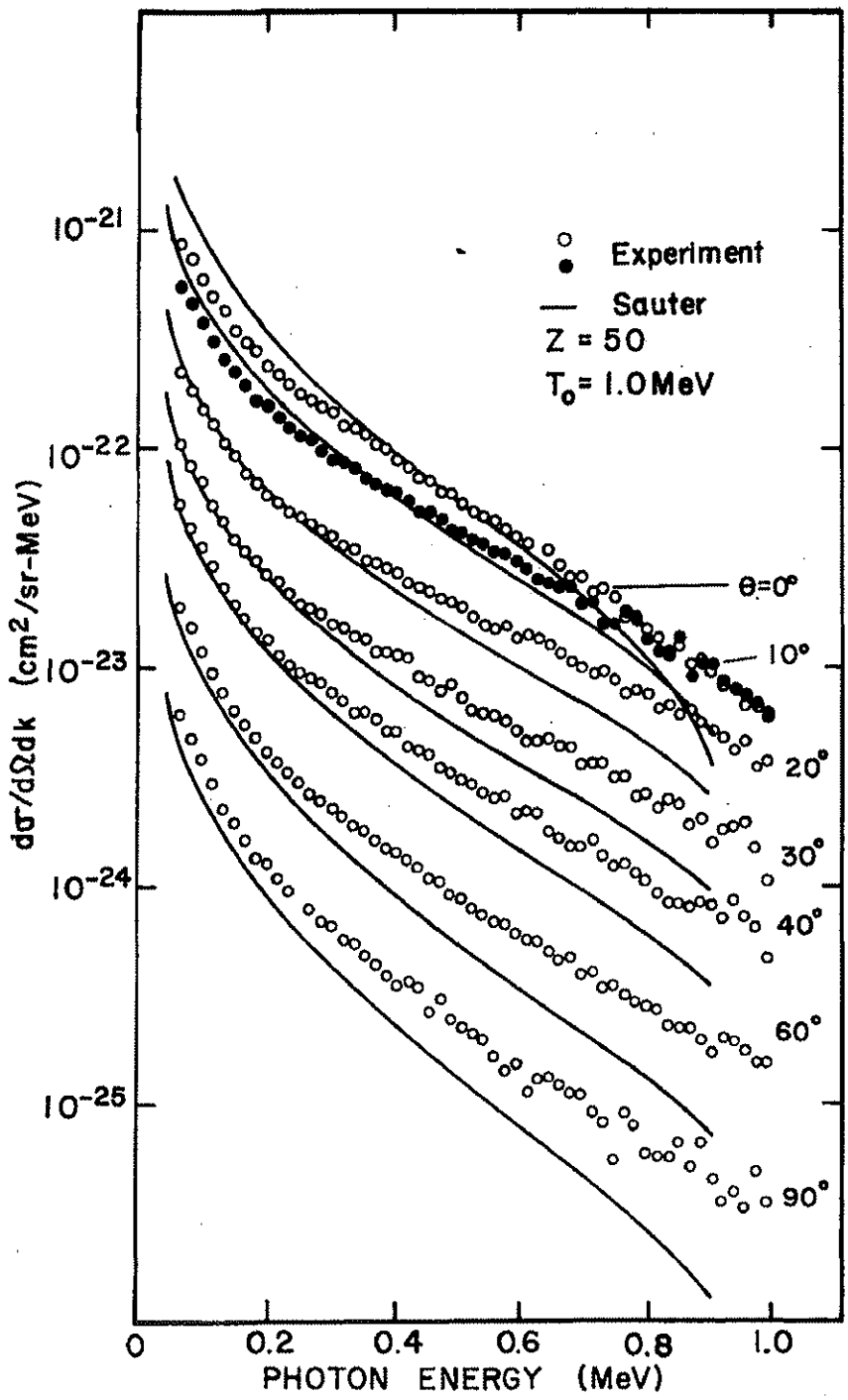

Figure 21. Bremsstrahlung differential cross sections for 1.0-MeV electrons on Sn.

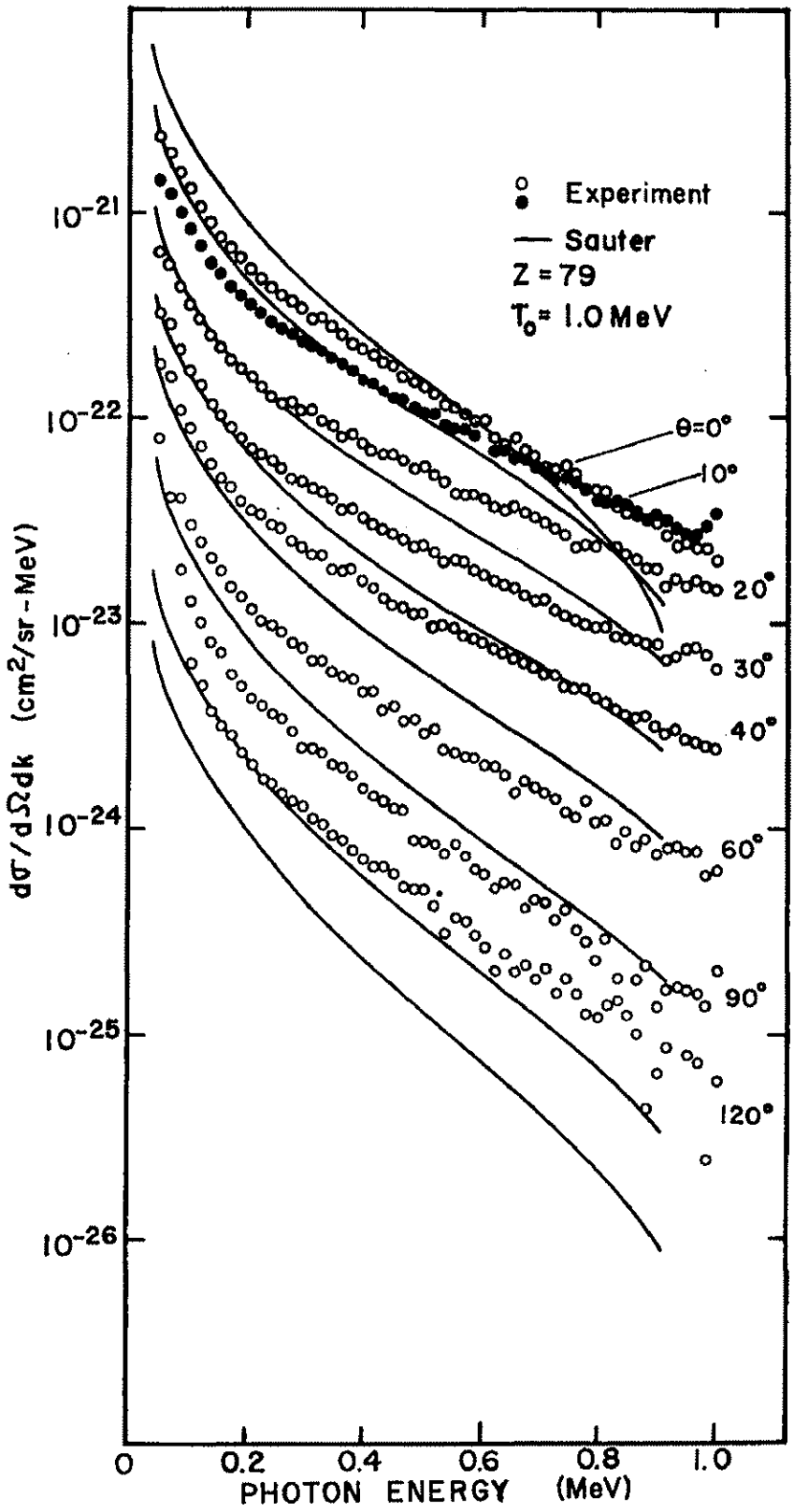

Figure 22. Bremsstrahlung differential cross sections for 1.0-MeV electrons on Au.

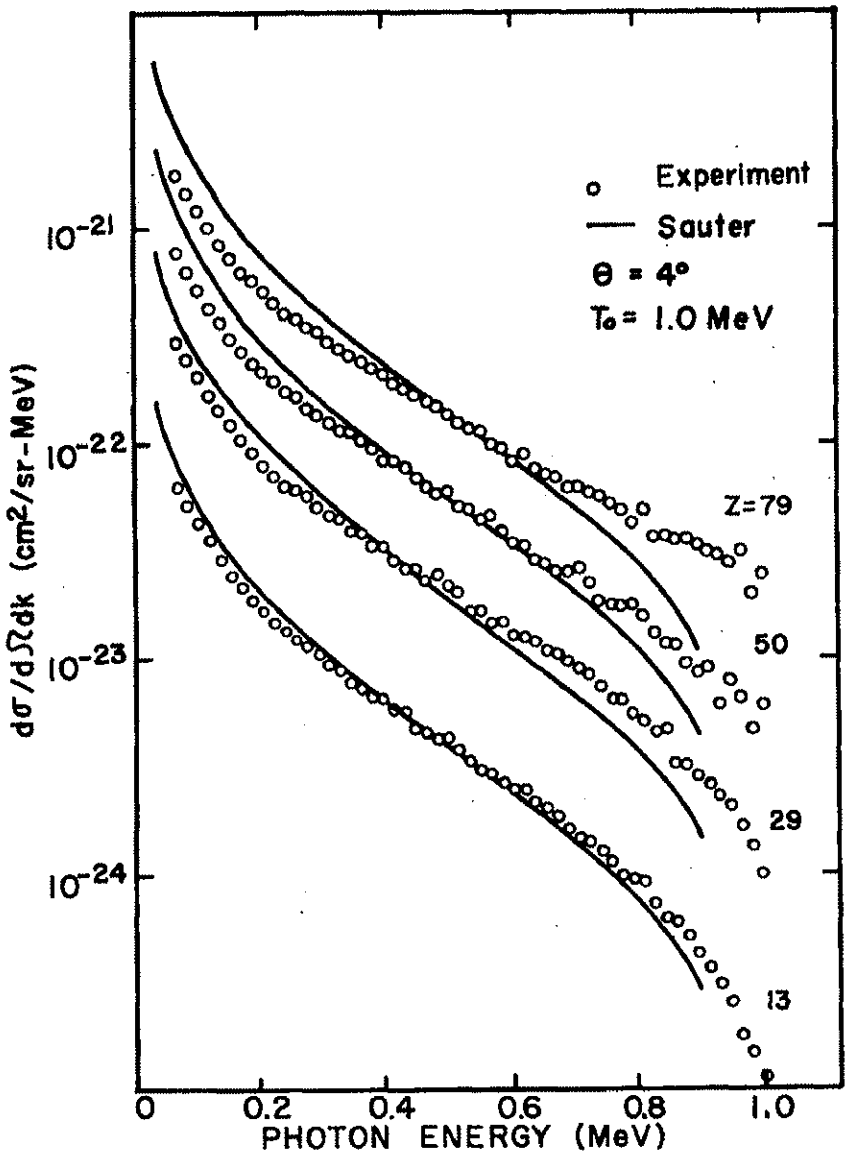

Figure 23. Bremsstrahlung differential cross sections, $\theta = 4$ deg, for 1.0-MeV electrons on Al, Cu, Sn, and Au.

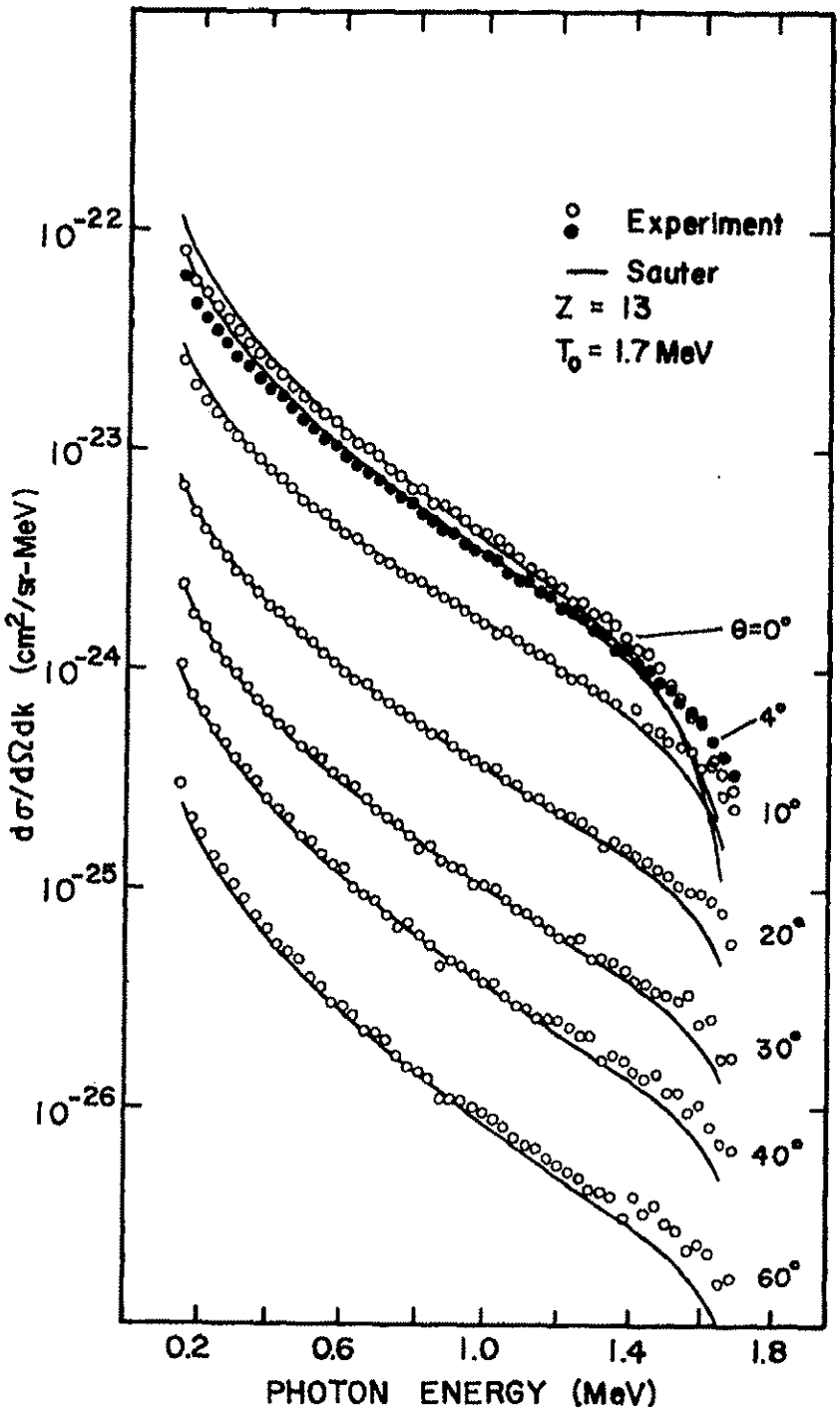

Figure 24. Bremsstrahlung differential cross sections for 1.7-MeV electrons on Al.

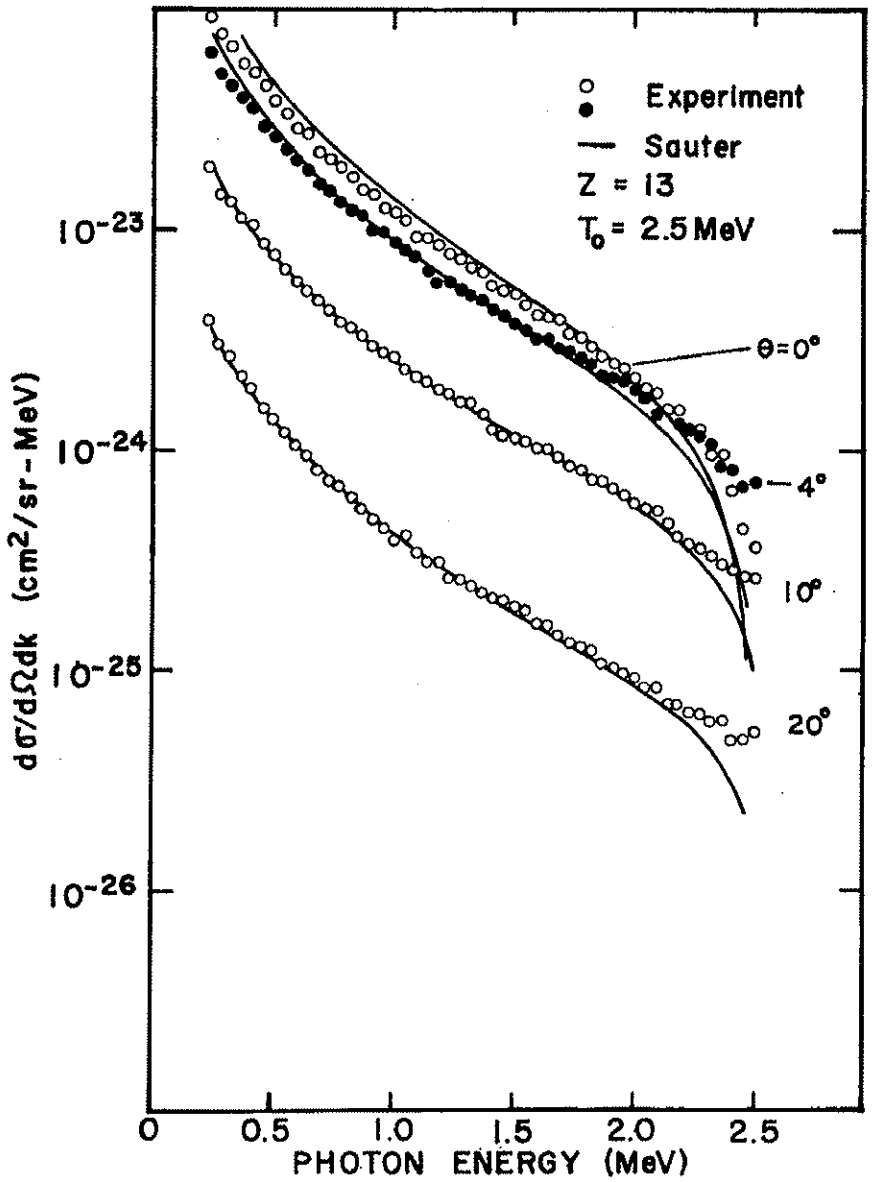

Figure 25. Bremsstrahlung differential cross sections for 2.5-MeV electrons on Al.

theory for the case of Al, except in the low and high photon energy regions of the spectra for all angles. However, with increasing atomic number of the target material the experimental spectra become relatively harder, as shown by the values for Cu, Sn, and Au. The measurements at T_o = 1.7 and 2.5 MeV for Al also indicate that the experiment and theory are in good agreement except in the low and high photon energy regions of the spectra. At 0 and 4 deg, however, the experimental values appear to be falling lower with increasing incident electron energy as compared to the Bethe-Heitler values.

The estimated average experimental error in the photon energy region $0.1\ T_o < k < 0.9\ T_o$ is about 15%. At 0 and 4 deg the error is estimated to be 7%. At larger angles additional uncertainty arises due to the angular uncertainty of 0.3 deg and the strong dependence of the yield on angle at angles greater than 10 deg. In the photon energy region greater than $k = 0.9\ T_o$ additional uncertainty arises due to the increased statistical error and the spectrometer response removal from the pulse height spectra. Thus the total error increases slowly in the region from $k = 0.9\ T_o$ to $0.95\ T_o$ and then more rapidly to about 30-50% at the end point value.

Various methods of spectrometer response removal from the pulse height spectra were attempted. The cross sections presented here have been obtained from the pulse height data normalized with respect to the spectrometer solid angle and the number of incident electrons by the following operations:

1. The hand-smoothed pulse height spectra were smeared by multiplying the spectra by the spectrometer response matrix.
2. The ratios of the smoothed pulse height spectra to the smeared spectra were computed.
3. The original unsmoothed pulse height spectra were multiplied by these ratios.
4. The spectra thus obtained were corrected for spectrometer efficiency.

The combined corrections applied to the pulse height spectra are shown in Fig. 26. Shown are examples for Au at $\theta = 0$ deg and $T_o = 1$ MeV and for Al at $\theta = 0$ deg and $T_o = 1$ MeV. The Au correction ratios are typical of the corrections made to most of the spectra. The Al correction factors differ from those of Au near the end point. This difference arises from the difference in the spectral shapes at the end point. Most of the spectra fall off sharply at the high energy end while at the forward angles 0 and 4 deg, the Al and Cu smoothly drop off in magnitude with considerably less curvature near the end point. This method of response removal was shown by use of test spectra to have an accuracy to within a few percent in the photon energy region below $k = 0.9\ T_o$. In the region $k > 0.95\ T_o$, however, this method tended to undercorrect the pulse height spectra by about 15% on the average. With the undercorrection taken into account there is still added uncertainty in the cross sections in the region $k > .9\ T_o$ reported here, since the corrections near the end point depend strongly on the detailed shape of the pulse height distribution in the pulse height region corresponding to $k > 0.75\ T_o$. Where many spectra are to be analyzed, as in the present case, it is impracticable to find the correction factors for each case because of the necessity for hand-smoothing the pulse height spectra. The present analysis consisted of finding the correction factors for classes of pulse height distribution shapes. Pulse height distributions in the various shape categories were then corrected by the appropriate set of factors for their class. Thus this procedure did not allow for the small differences within the shape classes.

Some of the spectra at each energy were accumulated with a Pb absorber, or beam hardener, in the photon beam between the target and spectrometer. The thickness of Pb was chosen to allow 85% or more transmission of photons with $k > 0.6\ T_o$ so that corrections due to the attenuation would be small. Running in this manner allowed improved statistics to be obtained in this region of the spectra, since relatively high beam currents could be run without distortion due to pulse pile-up. The cross sections obtained from data taken with the beam hardener are given in Table II. Statistical fluctuations in the 1-MeV data where this procedure was not followed are clearly evident.

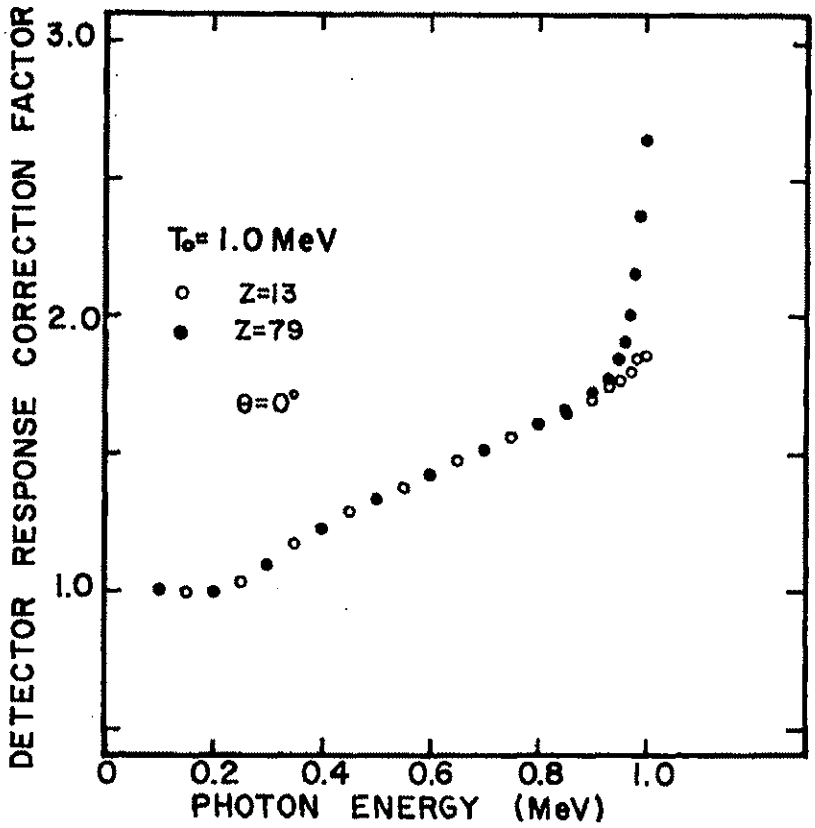

Figure 26. Examples of correction factors for removal of spectrometer response from the pulse height spectra.

The details of the x-ray spectrometer and its calibration and the scattering geometry have been presented in previous reports including NASA Contractor Report NASA CR-334. The only modification in the present experiment was to include provision for bending the electron beam after it passed through the target so that the electrons could be separated from the photon beam at the forward angles. This was done with a permanent magnet which deflected the beam into a shielded Faraday cup. The 0-deg direction for the incident electron beam was determined by mapping with the spectrometer the bremsstrahlung field in the region of its maximum in the forward direction.

REFERENCES

1. "Investigations of Electron Interactions With Matter," by William E. Dance, et al., NASA CR-334, 1965.
2. K. Wright and J. Trump, J. Appl. Phys. 33,(1962).
3. "Theoretical Calculations of the Bremsstrahlung Cross Section," Union Carbide Corporation Report UCC/DSSD-206.
4. H. W. Koch and J. W. Motz, Rev. Mod. Phys. 31, (1959).

TABLE I

EXPERIMENTAL ELECTRON-BREMSSTRAHLUNG CROSS SECTIONS

Z = 13

T_o = 1.0 MeV

k (MeV)	$d\sigma/d\Omega dk$ (cm^2/sr-MeV)		
θ =	0°	4°	10°
0.079	7.00(-23)	6.36(-23)	3.94(-23)
0.096	5.68(-23)	5.12(-23)	3.19(-23)
0.113	4.77(-23)	4.31(-23)	2.63(-23)
0.130	3.87(-23)	3.54(-23)	2.16(-23)
0.147	3.21(-23)	2.89(-23)	1.80(-23)
0.164	2.71(-23)	2.45(-23)	1.55(-23)
0.181	2.35(-23)	2.16(-23)	1.33(-23)
0.198	2.09(-23)	1.89(-23)	1.19(-23)
0.215	1.85(-23)	1.68(-23)	1.06(-23)
0.233	1.69(-23)	1.48(-23)	9.69(-24)
0.250	1.50(-23)	1.34(-23)	8.59(-24)
0.267	1.41(-23)	1.22(-23)	8.10(-24)
0.284	1.21(-23)	1.14(-23)	7.30(-24)
0.301	1.19(-23)	1.05(-23)	6.79(-24)
0.318	1.06(-23)	9.51(-24)	6.27(-24)
0.335	9.58(-24)	8.89(-24)	5.93(-24)
0.352	8.87(-24)	7.63(-24)	5.76(-24)
0.369	8.54(-24)	7.33(-24)	4.91(-24)
0.386	8.12(-24)	6.73(-24)	4.73(-24)
0.403	6.77(-24)	6.53(-24)	4.32(-24)
0.420	6.12(-24)	5.83(-24)	3.98(-24)
0.437	5.67(-24)	5.60(-24)	3.68(-24)
0.454	5.65(-24)	4.82(-24)	3.49(-24)
0.471	5.36(-24)	4.54(-24)	3.12(-24)
0.488	4.76(-24)	4.27(-24)	2.96(-24)
0.505	4.00(-24)	4.29(-24)	2.88(-24)
0.522	3.79(-24)	3.74(-24)	2.66(-24)
0.539	3.51(-24)	3.31(-24)	2.37(-24)
0.556	3.21(-24)	3.04(-24)	2.26(-24)
0.573	3.17(-24)	2.96(-24)	2.25(-24)
0.590	2.73(-24)	2.68(-24)	1.83(-24)
0.607	2.65(-24)	2.46(-24)	1.89(-24)
0.624	2.29(-24)	2.26(-24)	1.75(-24)
0.641	2.31(-24)	1.84(-24)	1.62(-24)
0.659	2.08(-24)	1.86(-24)	1.58(-24)
0.676	1.91(-24)	1.67(-24)	1.40(-24)
0.693	1.79(-24)	1.54(-24)	1.25(-24)
0.710	1.62(-24)	1.51(-24)	1.18(-24)
0.727	1.33(-24)	1.43(-24)	1.16(-24)
0.744	1.35(-24)	1.27(-24)	8.96(-25)
0.761	1.19(-24)	1.20(-24)	1.03(-24)
0.778	1.01(-24)	1.04(-24)	7.73(-25)
0.795	8.09(-25)	8.21(-25)	6.47(-25)
0.812	7.47(-25)	7.70(-25)	6.87(-25)
0.829	6.32(-25)	7.38(-25)	6.65(-25)
0.. 16	5.40(-25)	6.46(-25)	5.44(-25)
0.863	4.44(-25)	6.30(-25)	6.30(-25)
0.880	3.95(-25)	4.10(-25)	5.45(-25)
0.897	5.02(-25)	5.02(-25)	4.47(-25)
0.914	4.12(-25)	3.89(-25)	4.49(-25)
0.931	2.47(-25)	3.06(-25)	4.06(-25)
0.948	2.46(-25)	2.47(-25)	3.18(-25)
0.965	3.07(-25)	1.10(-25)	2.27(-25)
0.982	9.17(-26)	2.43(-25)	2.73(-25)
0.999	3.78(-26)	2.19(-25)	2.33(-25)

TABLE I (Continued)

Z = 13

T_o = 1.0 MeV

k (MeV)	dσ/dΩdk (cm^2/sr-MeV)			
θ =	20°	30°	40°	60°
0.079	1.45(-23)	6.49(-24)	3.36(-24)	1.12(-24)
0.096	1.18(-23)	5.15(-24)	2.62(-24)	8.71(-25)
0.113	9.75(-24)	4.21(-24)	2.06(-24)	6.66(-25)
0.130	7.92(-24)	3.41(-24)	1.62(-24)	5.17(-25)
0.147	6.63(-24)	2.91(-24)	1.36(-24)	4.19(-25)
0.164	5.39(-24)	2.40(-24)	1.12(-24)	3.52(-25)
0.181	4.96(-24)	2.05(-24)	9.65(-25)	2.87(-25)
0.198	4.29(-24)	1.75(-24)	8.80(-25)	2.58(-25)
0.215	3.88(-24)	1.61(-24)	7.63(-25)	2.23(-25)
0.233	3.55(-24)	1.42(-24)	6.50(-25)	1.99(-25)
0.250	3.23(-24)	1.32(-24)	5.93(-25)	1.73(-25)
0.267	3.00(-24)	1.23(-24)	5.54(-25)	1.58(-25)
0.284	2.83(-24)	1.07(-24)	4.92(-25)	1.46(-25)
0.301	2.62(-24)	9.90(-25)	4.50(-25)	1.24(-25)
0.318	2.36(-24)	9.26(-25)	4.05(-25)	1.12(-25)
0.335	2.30(-24)	8.33(-25)	3.76(-25)	1.06(-25)
0.352	2.05(-24)	7.61(-25)	3.43(-25)	9.92(-26)
0.369	1.86(-24)	7.78(-25)	3.30(-25)	8.69(-26)
0.386	1.73(-24)	6.46(-25)	3.06(-25)	7.72(-26)
0.403	1.70(-24)	6.27(-25)	2.64(-25)	7.41(-26)
0.420	1.62(-24)	5.72(-25)	2.49(-25)	6.76(-26)
0.437	1.44(-24)	5.54(-25)	2.28(-25)	6.36(-26)
0.454	1.41(-24)	5.17(-25)	2.07(-25)	5.87(-26)
0.471	1.22(-24)	4.83(-25)	1.94(-25)	5.41(-26)
0.488	1.25(-24)	4.63(-25)	1.95(-25)	4.72(-26)
0.505	1.17(-24)	4.33(-25)	1.49(-25)	4.59(-26)
0.522	1.02(-24)	3.69(-25)	1.54(-25)	3.89(-26)
0.539	1.00(-24)	3.70(-25)	1.64(-25)	3.84(-26)
0.556	8.97(-25)	3.42(-25)	1.30(-25)	3.55(-26)
0.573	8.55(-25)	3.19(-25)	1.09(-25)	3.34(-26)
0.590	8.01(-25)	2.78(-25)	1.21(-25)	2.80(-26)
0.607	7.98(-25)	2.72(-25)	1.09(-25)	2.55(-26)
0.624	7.58(-25)	2.53(-25)	8.68(-26)	2.72(-26)
0.641	6.90(-25)	2.46(-25)	9.77(-26)	2.16(-26)
0.659	5.95(-25)	2.34(-25)	8.79(-26)	1.97(-26)
0.676	5.71(-25)	2.08(-25)	8.06(-26)	2.31(-26)
0.693	5.74(-25)	1.96(-25)	7.55(-26)	1.75(-26)
0.710	4.96(-25)	1.64(-25)	6.87(-26)	1.70(-26)
0.727	4.67(-25)	1.60(-25)	7.67(-26)	1.78(-26)
0.744	4.64(-25)	1.51(-25)	6.78(-26)	1.43(-26)
0.761	4.28(-25)	1.37(-25)	6.15(-26)	1.43(-26)
0.778	3.77(-25)	1.44(-25)	5.30(-26)	1.39(-26)
0.795	3.23(-25)	1.22(-25)	4.40(-26)	1.04(-26)
0.812	3.78(-25)	1.26(-25)	4.10(-26)	8.57(-27)
0.829	2.80(-25)	1.00(-25)	3.75(-26)	8.72(-27)
0.846	2.73(-25)	9.23(-26)	4.10(-26)	9.26(-27)
0.863	2.82(-25)	8.97(-26)	4.14(-26)	8.32(-27)
0.880	2.64(-25)	9.46(-26)	3.49(-26)	8.65(-27)
0.897	2.35(-25)	6.67(-26)	3.13(-26)	4.17(-27)
0.914	2.21(-25)	7.17(-26)	3.05(-26)	5.79(-27)
0.931	2.29(-25)	7.86(-26)	2.36(-26)	6.12(-27)
0.948	1.73(-25)	5.63(-26)	3.14(-26)	4.85(-27)
0.965	1.52(-25)	5.36(-26)	2.90(-26)	3.75(-27)
0.982	1.20(-25)	5.46(-26)	1.77(-26)	5.06(-27)
0.999	1.05(-25)	4.71(-26)	9.32(-27)	1.40(-27)

TABLE I (Continued)

Z = 29

T_o = 1.0 MeV

k (MeV)	dσ/dΩdk (cm^2/sr-MeV)		
θ =	0°	4°	10°
0.079	3.35(-22)	2.95(-22)	1.99(-22)
0.096	1.98(-20)	2.43(-22)	1.64(-22)
0.113	2.26(-22)	2.04(-22)	1.37(-22)
0.130	1.89(-22)	1.65(-22)	1.14(-22)
0.147	1.60(-22)	1.41(-22)	9.54(-23)
0.164	1.33(-22)	1.21(-22)	8.05(-23)
0.181	1.17(-22)	1.02(-22)	7.10(-23)
0.198	1.00(-22)	9.06(-23)	6.09(-23)
0.215	9.01(-23)	7.86(-23)	5.52(-23)
0.233	7.94(-23)	7.16(-23)	5.17(-23)
0.250	7.38(-23)	6.29(-23)	4.56(-23)
0.267	6.78(-23)	6.07(-23)	4.22(-23)
0.284	6.51(-23)	5.76(-23)	3.91(-23)
0.301	5.68(-23)	5.02(-23)	3.64(-23)
0.318	5.45(-23)	4.61(-23)	3.36(-23)
0.335	4.86(-23)	4.47(-23)	3.16(-23)
0.352	4.56(-23)	3.90(-23)	2.98(-23)
0.369	3.89(-23)	3.87(-23)	2.65(-23)
0.386	3.77(-23)	3.36(-23)	2.51(-23)
0.403	3.56(-23)	3.31(-23)	2.30(-23)
0.420	3.36(-23)	2.84(-23)	2.26(-23)
0.437	2.89(-23)	2.62(-23)	2.07(-23)
0.454	2.70(-23)	2.58(-23)	1.92(-23)
0.471	2.58(-23)	2.30(-23)	1.74(-23)
0.488	2.36(-23)	2.42(-23)	1.68(-23)
0.505	2.35(-23)	2.17(-23)	1.49(-23)
0.522	2.05(-23)	2.02(-23)	1.49(-23)
0.539	1.90(-23)	1.66(-23)	1.35(-23)
0.556	1.84(-23)	1.65(-23)	1.31(-23)
0.573	1.70(-23)	1.44(-23)	1.24(-23)
0.590	1.33(-23)	1.45(-23)	1.06(-23)
0.607	1.35(-23)	1.28(-23)	9.95(-24)
0.624	1.26(-23)	1.08(-23)	9.56(-24)
0.641	1.18(-23)	1.12(-23)	9.08(-24)
0.659	9.77(-24)	1.06(-23)	8.10(-24)
0.676	1.05(-23)	7.95(-24)	8.09(-24)
0.693	8.32(-24)	9.85(-24)	7.08(-24)
0.710	7.82(-24)	8.87(-24)	6.87(-24)
0.727	7.67(-24)	6.80(-24)	7.13(-24)
0.744	7.66(-24)	7.18(-24)	5.89(-24)
0.761	5.26(-24)	5.44(-24)	5.50(-24)
0.778	5.93(-24)	5.16(-24)	5.01(-24)
0.795	5.37(-24)	5.63(-24)	4.73(-24)
0.812	4.97(-24)	4.83(-24)	4.41(-24)
0.829	3.87(-24)	4.46(-24)	4.28(-24)
0.846	3.90(-24)	4.10(-24)	4.02(-24)
0.863	3.70(-24)	3.60(-24)	3.92(-24)
0.880	2.73(-24)	3.23(-24)	3.29(-24)
0.897	2.16(-24)	2.88(-24)	3.39(-24)
0.914	1.97(-24)	1.96(-24)	2.88(-24)
0.931	1.92(-24)	1.95(-24)	3.16(-24)
0.948	1.47(-24)	1.88(-24)	2.55(-24)
0.965	1.70(-24)	1.33(-24)	2.39(-24)
0.982	9.40(-25)	1.26(-24)	1.47(-24)
0.999	6.00(-25)	9.94(-25)	1.28(-24)

TABLE I (Continued)

Z = 29

T_o = 1.0 MeV

k = (MeV	dσ/dΩdk (cm^2/sr-MeV)			
θ =	20°	30°	40°	60°
0.079	7.78(-23)	3.61(-23)	1.82(-23)	5.87(-24)
0.096	6.59(-23)	2.90(-23)	1.45(-23)	4.69(-24)
0.113	5.58(-23)	2.38(-23)	1.18(-23)	3.70(-24)
0.130	4.52(-23)	1.95(-23)	9.76(-24)	2.91(-24)
0.147	3.83(-23)	1.62(-23)	7.92(-24)	2.46(-24)
0.164	3.20(-23)	1.40(-23)	6.54(-24)	2.10(-24)
0.181	2.82(-23)	1.21(-23)	5.90(-24)	1.72(-24)
0.198	2.50(-23)	1.04(-23)	4.98(-24)	1.44(-24)
0.215	2.32(-23)	9.03(-24)	4.51(-24)	1.37(-24)
0.233	2.07(-23)	8.49(-24)	3.99(-24)	1.17(-24)
0.250	1.89(-23)	7.72(-24)	3.64(-24)	1.05(-24)
0.267	1.71(-23)	7.18(-24)	3.28(-24)	8.62(-25)
0.284	1.61(-23)	6.40(-24)	3.02(-24)	9.38(-25)
0.301	1.51(-23)	6.04(-24)	2.81(-24)	7.94(-25)
0.318	1.31(-23)	5.74(-24)	2.58(-24)	6.66(-25)
0.335	1.35(-23)	5.17(-24)	2.45(-24)	6.87(-25)
0.352	1.17(-23)	4.94(-24)	2.20(-24)	6.23(-25)
0.369	1.10(-23)	4.45(-24)	1.98(-24)	5.39(-25)
0.386	1.04(-23)	4.13(-24)	1.86(-24)	5.07(-25)
0.403	1.03(-23)	4.20(-24)	1.73(-24)	5.15(-25)
0.420	9.21(-24)	3.74(-24)	1.51(-24)	4.21(-25)
0.437	8.53(-24)	3.24(-24)	1.37(-24)	4.19(-25)
0.454	7.97(-24)	3.29(-24)	1.34(-24)	3.86(-25)
0.471	8.59(-24)	2.86(-24)	1.20(-24)	3.08(-25)
0.488	6.67(-24)	2.74(-24)	1.27(-24)	2.15(-25)
0.505	6.39(-24)	2.67(-24)	1.08(-24)	3.11(-25)
0.522	6.30(-24)	2.17(-24)	1.11(-24)	2.97(-25)
0.539	5.49(-24)	2.47(-24)	1.04(-24)	2.07(-25)
0.556	5.88(-24)	2.07(-24)	9.36(-25)	2.38(-25)
0.573	5.31(-24)	1.79(-24)	9.03(-25)	2.09(-25)
0.590	4.52(-24)	2.13(-24)	7.91(-25)	2.37(-25)
0.607	4.47(-24)	1.50(-24)	7.00(-25)	1.59(-25)
0.624	4.37(-24)	1.53(-24)	6.83(-25)	1.54(-25)
0.641	4.27(-24)	1.40(-24)	7.12(-25)	1.56(-25)
0.659	4.04(-24)	1.25(-24)	5.62(-25)	1.62(-25)
0.676	3.79(-24)	1.43(-24)	6.11(-25)	1.54(-25)
0.693	3.05(-24)	1.30(-24)	5.07(-25)	1.54(-25)
0.710	3.48(-24)	1.06(-24)	4.24(-25)	1.01(-25)
0.727	2.81(-24)	1.25(-24)	4.60(-25)	8.36(-26)
0.744	3.28(-24)	1.13(-24)	3.90(-25)	9.78(-26)
0.761	2.85(-24)	9.07(-25)	3.60(-25)	6.91(-26)
0.778	2.60(-24)	9.77(-25)	3.59(-25)	8.60(-26)
0.795	2.41(-24)	8.47(-25)	3.96(-25)	8.71(-26)
0.812	1.78(-24)	4.27(-25)	3.13(-25)	9.23(-26)
0.829	2.28(-24)	6.51(-25)	3.18(-25)	6.91(-26)
0.846	1.89(-24)	7.24(-25)	2.79(-25)	5.71(-26)
0.863	1.63(-24)	6.66(-25)	2.85(-25)	7.80(-26)
0.880	1.65(-24)	7.35(-25)	3.08(-25)	5.70(-26)
0.897	1.40(-24)	4.94(-25)	2.35(-25)	7.54(-26)
0.914	1.43(-24)	5.71(-25)	2.23(-25)	4.80(-26)
0.931	1.43(-24)	4.16(-25)	2.04(-25)	5.51(-26)
0.948	1.18(-24)	4.46(-25)	1.91(-25)	3.79(-26)
0.965	1.20(-24)	4.95(-25)	1.73(-25)	1.33(-26)
0.982	1.00(-24)	4.32(-25)	1.62(-25)	3.64(-26)
0.999	1.24(-24)	5.89(-25)	9.69(-26)	4.34(-26)

TABLE I (Continued)

Z = 50

T_o = 1.0 MeV

k (MeV)	dσ/dΩdk (cm^2/sr-MeV)			
θ =	0°	4°	10°	20°
0.079	8.28(-22)	7.68(-22)	5.16(-22)	2.10(-22)
0.096	6.84(-22)	6.36(-22)	4.25(-22)	1.73(-22)
0.113	5.64(-22)	5.19(-22)	3.47(-22)	1.44(-22)
0.130	4.64(-22)	4.22(-22)	2.88(-22)	1.19(-22)
0.147	3.95(-22)	3.64(-22)	2.40(-22)	9.72(-23)
0.164	3.33(-22)	3.10(-22)	2.09(-22)	8.57(-23)
0.181	2.93(-22)	2.67(-22)	1.83(-22)	7.46(-23)
0.198	2.60(-22)	2.35(-22)	1.60(-22)	6.58(-23)
0.215	2.28(-22)	2.15(-22)	1.46(-22)	5.93(-23)
0.233	2.09(-22)	1.93(-22)	1.34(-22)	5.43(-23)
0.250	1.88(-22)	1.73(-22)	1.18(-22)	5.04(-23)
0.267	1.73(-22)	1.65(-22)	1.16(-22)	4.58(-23)
0.284	1.66(-22)	1.47(-22)	1.03(-22)	4.47(-23)
0.301	1.52(-22)	1.38(-22)	9.58(-23)	4.09(-23)
0.318	1.32(-22)	1.26(-22)	8.59(-23)	3.86(-23)
0.335	1.27(-22)	1.14(-22)	8.48(-23)	3.48(-23)
0.352	1.19(-22)	1.13(-22)	7.89(-23)	3.39(-23)
0.369	1.11(-22)	1.02(-22)	7.01(-23)	3.01(-23)
0.386	1.02(-22)	9.41(-23)	6.83(-23)	2.91(-23)
0.403	9.65(-23)	8.40(-23)	6.50(-23)	2.77(-23)
0.420	8.65(-23)	8.30(-23)	6.03(-23)	2.58(-23)
0.437	7.46(-23)	7.63(-23)	5.57(-23)	2.37(-23)
0.454	7.52(-23)	6.98(-23)	4.83(-23)	2.29(-23)
0.471	6.78(-23)	6.36(-23)	5.17(-23)	2.24(-23)
0.488	6.25(-23)	5.99(-23)	4.64(-23)	1.99(-23)
0.505	5.97(-23)	5.96(-23)	4.00(-23)	1.98(-23)
0.522	5.83(-23)	5.07(-23)	4.09(-23)	1.81(-23)
0.539	4.87(-23)	4.88(-23)	3.77(-23)	1.61(-23)
0.556	4.78(-23)	4.41(-23)	3.52(-23)	1.63(-23)
0.573	4.44(-23)	4.59(-23)	3.47(-23)	1.46(-23)
0.590	4.27(-23)	3.92(-23)	3.17(-23)	1.52(-23)
0.607	3.89(-23)	3.47(-23)	2.75(-23)	1.34(-23)
0.624	3.41(-23)	3.37(-23)	3.01(-23)	1.36(-23)
0.641	3.17(-23)	2.85(-23)	2.41(-23)	1.29(-23)
0.659	3.29(-23)	2.72(-23)	2.41(-23)	1.24(-23)
0.676	3.00(-23)	2.55(-23)	2.35(-23)	1.10(-23)
0.693	2.50(-23)	2.50(-23)	2.15(-23)	1.05(-23)
0.710	2.27(-23)	2.60(-23)	1.94(-23)	9.48(-24)
0.727	2.27(-23)	2.25(-23)	1.87(-23)	1.00(-23)
0.744	2.30(-23)	1.82(-23)	1.60(-23)	9.26(-24)
0.761	1.80(-23)	1.79(-23)	1.64(-23)	8.56(-24)
0.778	1.65(-23)	1.76(-23)	1.71(-23)	7.05(-24)
0.795	1.60(-23)	1.78(-23)	1.65(-23)	7.36(-24)
0.812	1.35(-23)	1.58(-23)	1.14(-23)	6.99(-24)
0.829	1.36(-23)	1.30(-23)	1.23(-23)	6.60(-24)
0.846	1.19(-23)	1.19(-23)	1.25(-23)	6.44(-24)
0.863	1.21(-23)	1.14(-23)	1.10(-23)	6.10(-24)
0.880	9.60(-24)	9.47(-24)	9.74(-24)	6.05(-24)
0.897	1.08(-23)	8.57(-24)	9.78(-24)	5.35(-24)
0.914	8.94(-24)	9.05(-24)	9.76(-24)	5.07(-24)
0.931	6.61(-24)	6.12(-24)	8.04(-24)	4.49(-24)
0.948	3.71(-24)	7.94(-24)	7.64(-24)	4.19(-24)
0.965	5.58(-24)	6.61(-24)	7.36(-24)	4.39(-24)
0.982	6.40(-24)	4.77(-24)	6.49(-24)	3.46(-24)
0.999	5.15(-24)	6.11(-24)	5.74(-24)	3.53(-24)

TABLE I (Continued)

Z = 50

T_o = 1.0 MeV

k (MeV)	dσ/dΩdk (cm²/sr-MeV)			
θ =	30°	40°	60°	90°
0.079	9.69(-23)	5.15(-23)	1.77(-23)	5.55(-24)
0.096	7.80(-23)	4.00(-23)	1.38(-23)	4.31(-24)
0.113	6.39(-23)	3.20(-23)	1.08(-23)	3.45(-24)
0.130	5.20(-23)	2.62(-23)	8.83(-24)	2.67(-24)
0.147	4.25(-23)	2.13(-23)	7.17(-24)	2.20(-24)
0.164	3.66(-23)	1.83(-23)	5.87(-24)	1.78(-24)
0.181	3.24(-23)	1.57(-23)	5.16(-24)	1.49(-24)
0.198	2.88(-23)	1.41(-23)	4.54(-24)	1.29(-24)
0.215	2.57(-23)	1.23(-23)	3.90(-24)	1.20(-24)
0.233	2.31(-23)	1.11(-23)	3.47(-24)	1.03(-24)
0.250	2.10(-23)	9.83(-24)	3.22(-24)	9.36(-25)
0.267	1.91(-23)	9.10(-24)	2.83(-24)	8.69(-25)
0.284	1.81(-23)	8.62(-24)	2.54(-24)	7.51(-25)
0.301	1.68(-23)	8.18(-24)	2.36(-24)	6.63(-25)
0.318	1.57(-23)	7.30(-24)	2.18(-24)	6.08(-25)
0.335	1.43(-23)	6.65(-24)	2.01(-24)	6.01(-25)
0.352	1.36(-23)	6.31(-24)	1.82(-24)	5.16(-25)
0.369	1.26(-23)	6.00(-24)	1.72(-24)	4.56(-25)
0.386	1.16(-23)	5.35(-24)	1.56(-24)	4.20(-25)
0.403	1.17(-23)	5.15(-24)	1.44(-24)	3.43(-25)
0.420	1.06(-23)	4.77(-24)	1.36(-24)	3.59(-25)
0.437	9.86(-24)	4.18(-24)	1.29(-24)	3.50(-25)
0.454	8.99(-24)	4.06(-24)	1.18(-24)	3.35(-25)
0.471	7.96(-24)	3.86(-24)	1.06(-24)	2.63(-25)
0.488	8.33(-24)	3.50(-24)	9.50(-25)	2.86(-25)
0.505	7.92(-24)	3.12(-24)	8.85(-25)	2.51(-25)
0.522	7.04(-24)	3.09(-24)	8.74(-25)	2.44(-25)
0.539	6.49(-24)	2.77(-24)	7.69(-25)	1.73(-25)
0.556	6.04(-24)	2.61(-24)	7.41(-25)	2.11(-25)
0.573	5.99(-24)	2.56(-24)	7.07(-25)	1.40(-25)
0.590	5.18(-24)	2.31(-24)	6.17(-25)	1.37(-25)
0.607	5.21(-24)	2.18(-24)	5.79(-25)	1.56(-25)
0.624	4.31(-24)	2.11(-24)	5.82(-25)	1.18(-25)
0.641	4.62(-24)	2.21(-24)	5.45(-25)	1.31(-25)
0.659	4.93(-24)	1.59(-24)	4.77(-25)	1.19(-25)
0.676	3.91(-24)	1.60(-24)	4.42(-25)	1.16(-25)
0.693	4.20(-24)	1.53(-24)	4.60(-25)	1.16(-25)
0.710	3.63(-24)	1.61(-24)	3.83(-25)	9.25(-26)
0.727	3.56(-24)	1.53(-24)	3.81(-25)	1.02(-25)
0.744	3.36(-24)	1.32(-24)	3.40(-25)	8.10(-26)
0.761	3.18(-24)	1.19(-24)	3.39(-25)	5.49(-26)
0.778	2.88(-24)	1.22(-24)	3.10(-25)	9.95(-26)
0.795	2.49(-24)	1.09(-24)	2.97(-25)	5.60(-26)
0.812	2.45(-24)	1.03(-24)	2.52(-25)	6.35(-26)
0.829	2.62(-24)	9.14(-25)	2.75(-25)	5.17(-26)
0.846	2.31(-24)	8.53(-25)	2.20(-25)	6.29(-26)
0.863	2.11(-24)	8.07(-25)	2.34(-25)	6.48(-26)
0.880	2.00(-24)	8.17(-25)	1.91(-25)	4.87(-26)
0.897	1.67(-24)	8.40(-25)	1.95(-25)	7.19(-26)
0.914	1.61(-24)	7.03(-25)	1.89(-25)	3.25(-26)
0.931	1.93(-24)	7.00(-25)	1.94(-25)	4.21(-26)
0.948	1.66(-24)	8.73(-25)	1.79(-25)	3.49(-26)
0.965	1.82(-24)	6.77(-25)	1.74(-25)	3.86(-26)
0.982	1.36(-24)	6.25(-25)	1.65(-25)	4.64(-26)
0.999	8.87(-25)	2.84(-25)	1.35(-25)	3.40(-26)

TABLE I (Continued)

Z = 79

T_o = 1.0 MeV

k (MeV)	dσ/dΩdk (cm^2/sr-MeV)			
	θ = 0°	4°	10°	20°
0.079	1.93(-21)	1.78(-21)	1.22(-21)	5.65(-22)
0.096	1.57(-21)	1.44(-21)	9.98(-22)	4.51(-22)
0.113	1.33(-21)	1.19(-21)	8.27(-22)	3.64(-22)
0.130	1.07(-21)	1.01(-21)	6.84(-22)	3.04(-22)
0.147	9.08(-22)	8.36(-22)	5.74(-22)	2.60(-22)
0.164	7.73(-22)	7.24(-22)	5.01(-22)	2.24(-22)
0.181	6.71(-22)	6.28(-22)	4.34(-22)	1.93(-22)
0.198	6.08(-22)	5.67(-22)	3.90(-22)	1.74(-22)
0.215	5.42(-22)	5.07(-22)	3.56(-22)	1.61(-22)
0.233	4.81(-22)	4.49(-22)	3.21(-22)	1.42(-22)
0.250	4.38(-22)	4.02(-22)	2.94(-22)	1.28(-22)
0.267	4.04(-22)	3.75(-22)	2.72(-22)	1.20(-22)
0.284	3.77(-22)	3.46(-22)	2.52(-22)	1.20(-22)
0.301	3.42(-22)	3.30(-22)	2.36(-22)	1.09(-22)
0.318	3.15(-22)	2.98(-22)	2.25(-22)	1.03(-22)
0.335	3.07(-22)	2.75(-22)	2.10(-22)	9.62(-23)
0.352	2.82(-22)	2.55(-22)	1.91(-22)	9.22(-23)
0.369	2.59(-22)	2.35(-22)	1.82(-22)	8.20(-23)
0.386	2.29(-22)	2.20(-22)	1.69(-22)	8.49(-23)
0.403	2.15(-22)	2.07(-22)	1.56(-22)	7.66(-23)
0.420	2.00(-22)	1.89(-22)	1.47(-22)	7.10(-23)
0.437	1.88(-22)	1.79(-22)	1.35(-22)	6.75(-23)
0.454	1.78(-22)	1.68(-22)	1.26(-22)	6.70(-23)
0.471	1.62(-22)	1.56(-22)	1.23(-22)	6.30(-23)
0.488	1.51(-22)	1.50(-22)	1.14(-22)	5.69(-23)
0.505	1.44(-22)	1.37(-22)	1.07(-22)	5.88(-23)
0.522	1.36(-22)	1.23(-22)	1.06(-22)	5.33(-23)
0.539	1.19(-22)	1.17(-22)	9.22(-23)	4.99(-23)
0.556	1.16(-22)	1.13(-22)	8.85(-23)	4.35(-23)
0.573	1.06(-22)	9.87(-23)	8.78(-23)	4.25(-23)
0.590	9.87(-23)	9.47(-23)	8.23(-23)	4.28(-23)
0.607	9.91(-23)	8.33(-23)	8.01(-23)	4.05(-23)
0.624	8.26(-23)	8.90(-23)	6.98(-23)	3.82(-23)
0.641	8.31(-23)	7.60(-23)	7.07(-23)	3.55(-23)
0.659	8.19(-23)	7.04(-23)	6.51(-23)	3.78(-23)
0.676	7.14(-23)	6.84(-23)	6.31(-23)	3.48(-23)
0.693	6.65(-23)	6.36(-23)	5.76(-23)	3.32(-23)
0.710	5.93(-23)	6.35(-23)	5.67(-23)	3.14(-23)
0.727	5.69(-23)	5.96(-23)	4.93(-23)	2.97(-23)
0.744	5.81(-23)	5.70(-23)	5.02(-23)	2.68(-23)
0.761	5.42(-23)	5.25(-23)	4.99(-23)	2.31(-23)
0.778	4.64(-23)	4.84(-23)	4.50(-23)	2.37(-23)
0.795	4.57(-23)	4.27(-23)	3.94(-23)	2.38(-23)
0.812	4.43(-23)	4.87(-23)	3.89(-23)	2.48(-23)
0.829	3.76(-23)	3.69(-23)	3.91(-23)	2.33(-23)
0.846	3.54(-23)	3.72(-23)	3.76(-23)	2.17(-23)
0.863	3.56(-23)	3.54(-23)	3.46(-23)	2.05(-23)
0.880	3.27(-23)	3.58(-23)	3.24(-23)	1.85(-23)
0.897	3.06(-23)	3.34(-23)	3.44(-23)	1.80(-23)
0.914	2.71(-23)	3.10(-23)	3.19(-23)	1.52(-23)
0.931	2.40(-23)	3.02(-23)	2.88(-23)	1.67(-23)
0.948	2.47(-23)	2.77(-23)	2.77(-23)	1.57(-23)
0.965	2.35(-23)	3.11(-23)	2.75(-23)	1.64(-23)
0.982	2.33(-23)	1.99(-23)	3.12(-23)	1.51(-23)
0.999	2.07(-23)	2.43(-23)	3.44(-23)	1.48(-23)

TABLE I (Continued)

Z = 79

T_o = 1.0 MeV

k (MeV)	dσ/dΩdk (cm^2/sr-MeV)			
θ =	30°	40°	60°	90°
0.079	2.84(-22)	1.63(-22)	7.29(-23)	4.18(-23)
0.096	2.12(-22)	1.11(-22)	4.19(-23)	1.82(-23)
0.113	1.73(-22)	9.14(-23)	3.12(-23)	1.30(-23)
0.130	1.45(-22)	7.27(-23)	2.50(-23)	1.01(-23)
0.147	1.18(-22)	6.13(-23)	2.10(-23)	8.08(-24)
0.164	1.04(-22)	5.21(-23)	1.80(-23)	7.09(-24)
0.181	9.07(-23)	4.66(-23)	1.51(-23)	5.74(-24)
0.198	8.01(-23)	4.01(-23)	1.35(-23)	4.89(-24)
0.215	7.16(-23)	3.63(-23)	1.19(-23)	4.39(-24)
0.233	6.75(-23)	3.37(-23)	1.05(-23)	3.99(-24)
0.250	6.27(-23)	3.07(-23)	9.96(-24)	3.68(-24)
0.267	5.74(-23)	2.87(-23)	9.14(-24)	3.36(-24)
0.284	5.20(-23)	2.49(-23)	8.12(-24)	2.99(-24)
0.301	4.96(-23)	2.39(-23)	7.71(-24)	2.46(-24)
0.318	4.63(-23)	2.21(-23)	6.67(-24)	2.45(-24)
0.335	4.41(-23)	2.12(-23)	6.65(-24)	2.31(-24)
0.352	4.10(-23)	1.82(-23)	5.87(-24)	2.09(-24)
0.369	4.05(-23)	1.78(-23)	5.60(-24)	1.97(-24)
0.386	3.60(-23)	1.82(-23)	5.33(-24)	1.81(-24)
0.403	3.28(-23)	1.64(-23)	4.75(-24)	1.56(-24)
0.420	3.06(-23)	1.51(-23)	4.63(-24)	1.41(-24)
0.437	2.88(-23)	1.33(-23)	3.83(-24)	1.38(-24)
0.454	2.80(-23)	1.24(-23)	3.95(-24)	1.28(-24)
0.471	2.60(-23)	1.22(-23)	3.39(-24)	1.22(-24)
0.488	2.40(-23)	1.13(-23)	3.40(-24)	8.82(-25)
0.505	2.44(-23)	1.13(-23)	2.93(-24)	8.67(-25)
0.522	2.23(-23)	1.03(-23)	3.02(-24)	8.44(-25)
0.539	2.03(-23)	1.01(-23)	2.42(-24)	7.50(-25)
0.556	2.05(-23)	8.60(-24)	2.33(-24)	8.54(-25)
0.573	1.98(-23)	8.55(-24)	2.26(-24)	7.42(-25)
0.590	1.84(-23)	7.97(-24)	2.23(-24)	6.36(-25)
0.607	1.74(-23)	7.56(-24)	2.07(-24)	5.98(-25)
0.624	1.62(-23)	6.68(-24)	1.97(-24)	5.06(-25)
0.641	1.56(-23)	6.52(-24)	1.78(-24)	5.50(-25)
0.659	1.50(-23)	6.87(-24)	1.51(-24)	5.32(-25)
0.676	1.39(-23)	6.05(-24)	1.73(-24)	4.00(-25)
0.693	1.29(-23)	5.73(-24)	1.59(-24)	4.47(-25)
0.710	1.30(-23)	5.66(-24)	1.49(-24)	4.36(-25)
0.727	1.16(-23)	5.06(-24)	1.39(-24)	3.52(-25)
0.744	1.10(-23)	4.95(-24)	1.21(-24)	4.00(-25)
0.761	1.07(-23)	5.06(-24)	1.13(-24)	3.14(-25)
0.778	1.00(-23)	4.11(-24)	1.38(-24)	2.76(-25)
0.795	9.59(-23)	4.01(-24)	1.07(-24)	2.28(-25)
0.812	9.75(-24)	4.08(-24)	1.10(-24)	2.92(-25)
0.829	8.79(-24)	4.26(-24)	8.53(-25)	1.84(-25)
0.846	8.62(-24)	3.48(-24)	9.64(-25)	1.87(-25)
0.863	8.34(-24)	3.94(-24)	8.17(-25)	1.83(-25)
0.880	8.11(-24)	3.36(-24)	8.85(-25)	2.19(-25)
0.897	7.94(-24)	3.21(-24)	7.57(-25)	1.34(-25)
0.914	6.67(-24)	3.31(-24)	7.94(-25)	1.66(-25)
0.931	6.90(-24)	3.00(-24)	8.26(-25)	1.67(-25)
0.948	7.48(-24)	2.63(-24)	7.77(-25)	1.63(-25)
0.965	7.65(-24)	2.29(-24)	7.64(-25)	1.50(-25)
0.982	7.00(-24)	2.50(-24)	5.95(-25)	1.37(-25)
0.999	5.99(-24)	3.45(-24)	6.18(-25)	2.05(-25)

TABLE I (Continued)

Z = 79

T_o = 1.0 MeV

k (MeV)	$d\sigma/d\Omega dk$ (cm^2/sr-MeV)
θ = 120°	
0.079	3.99(-23)
0.096	1.58(-23)
0.113	1.10(-23)
0.130	8.32(-24)
0.147	5.96(-24)
0.164	5.31(-24)
0.181	4.17(-24)
0.198	3.83(-24)
0.215	3.16(-24)
0.233	2.87(-24)
0.250	2.63(-24)
0.267	2.30(-24)
0.284	1.92(-24)
0.301	1.89(-24)
0.318	1.72(-24)
0.335	1.48(-24)
0.352	1.53(-24)
0.369	1.19(-24)
0.386	9.91(-25)
0.403	9.79(-25)
0.420	9.85(-25)
0.437	8.32(-25)
0.454	7.07(-25)
0.471	6.60(-25)
0.488	6.76(-25)
0.505	7.62(-25)
0.522	5.30(-25)
0.539	5.04(-25)
0.556	5.33(-25)
0.573	3.29(-25)
0.590	4.55(-25)
0.607	3.22(-25)
0.624	2.29(-25)
0.641	2.87(-25)
0.659	3.39(-25)
0.676	2.58(-25)
0.693	1.47(-25)
0.710	5.07(-26)
0.727	1.50(-25)
0.744	8.21(-26)
0.761	8.30(-26)
0.778	7.44(-26)
0.795	6.92(-26)
0.812	1.27(-25)
0.829	7.37(-26)
0.846	6.15(-26)
0.863	8.18(-26)
0.880	2.99(-26)
0.897	6.71(-26)
0.914	3.49(-27)
0.931	5.21(-26)
0.948	1.08(-26)
0.965	2.61(-25)
0.982	3.84(-25)
0.999	5.55(-25)

TABLE I (Continued)

Z = 13

T_0 = 1.7 MeV

k (MeV)	dσ/dΩdk (cm^2/sr-MeV)			
	θ = 0°	4°	10°	20°
0.156	8.01(-23)	6.10(-23)	2.53(-23)	6.83(-24)
0.186	5.90(-23)	4.50(-23)	1.94(-23)	5.07(-24)
0.216	5.17(-23)	3.95(-23)	1.67(-23)	4.28(-24)
0.245	4.44(-23)	3.40(-23)	1.44(-23)	3.67(-24)
0.275	3.91(-23)	3.03(-23)	1.29(-23)	3.19(-24)
0.305	3.45(-23)	2.67(-23)	1.13(-23)	2.80(-24)
0.335	3.04(-23)	2.34(-23)	1.00(-23)	2.53(-24)
0.364	2.71(-23)	2.09(-23)	8.91(-24)	2.21(-24)
0.394	2.46(-23)	1.89(-23)	8.10(-24)	1.92(-24)
0.424	2.18(-23)	1.71(-23)	7.29(-24)	1.79(-24)
0.454	1.91(-23)	1.54(-23)	6.61(-24)	1.61(-24)
0.484	1.77(-23)	1.36(-23)	5.87(-24)	1.47(-24)
0.513	1.58(-23)	1.25(-23)	5.44(-24)	1.32(-24)
0.543	1.45(-23)	1.11(-23)	5.00(-24)	1.18(-24)
0.573	1.33(-23)	1.02(-23)	4.58(-24)	1.07(-24)
0.603	1.19(-23)	9.34(-24)	4.18(-24)	9.65(-25)
0.633	1.08(-23)	8.48(-24)	3.89(-24)	8.89(-25)
0.662	1.00(-23)	7.93(-24)	3.47(-24)	8.47(-25)
0.692	9.37(-24)	7.29(-24)	3.18(-24)	7.43(-25)
0.722	8.30(-24)	6.66(-24)	3.05(-24)	7.13(-25)
0.752	7.64(-24)	6.15(-24)	2.78(-24)	6.50(-25)
0.781	6.65(-24)	5.80(-24)	2.60(-24)	6.08(-25)
0.811	6.62(-24)	5.06(-24)	2.55(-24)	6.08(-25)
0.841	5.81(-24)	4.84(-24)	2.27(-24)	5.45(-25)
0.871	5.58(-24)	4.34(-24)	2.09(-24)	5.09(-25)
0.901	5.25(-24)	4.22(-24)	2.01(-24)	4.96(-25)
0.930	4.83(-24)	3.73(-24)	1.86(-24)	4.45(-25)
0.960	4.46(-24)	3.58(-24)	1.73(-24)	3.39(-25)
0.990	4.15(-24)	3.31(-24)	1.63(-24)	2.94(-25)
1.020	3.78(-24)	3.19(-24)	1.44(-24)	3.26(-25)
1.050	3.55(-24)	2.96(-24)	1.51(-24)	3.51(-25)
1.079	3.28(-24)	2.58(-24)	1.36(-24)	3.12(-25)
1.109	2.86(-24)	2.49(-24)	1.25(-24)	2.77(-25)
1.139	2.73(-24)	2.25(-24)	1.18(-24)	2.49(-25)
1.169	2.52(-24)	2.20(-24)	1.10(-24)	2.59(-25)
1.198	2.40(-24)	1.99(-24)	1.07(-24)	2.35(-25)
1.228	2.03(-24)	1.87(-24)	9.40(-25)	2.51(-25)
1.258	1.88(-24)	1.85(-24)	9.14(-25)	2.05(-25)
1.288	1.65(-24)	1.49(-24)	8.40(-25)	1.62(-25)
1.318	1.76(-24)	1.48(-24)	8.10(-25)	1.80(-25)
1.347	1.55(-24)	1.35(-24)	7.19(-25)	1.70(-25)
1.377	1.34(-24)	1.25(-24)	6.67(-25)	1.42(-25)
1.407	1.19(-24)	1.09(-24)	7.19(-25)	1.21(-25)
1.437	1.09(-24)	1.01(-24)	5.39(-25)	1.36(-25)
1.467	1.00(-24)	9.25(-25)	5.86(-25)	1.13(-25)
1.496	7.76(-25)	8.50(-25)	4.15(-25)	1.20(-25)
1.526	7.60(-25)	6.70(-25)	4.87(-25)	1.19(-25)
1.556	7.29(-25)	5.96(-25)	3.96(-25)	7.24(-26)
1.586	5.12(-25)	5.42(-25)	3.52(-25)	9.20(-26)
1.615	4.35(-25)	4.34(-25)	2.83(-25)	9.15(-26)
1.645	4.37(-25)	4.08(-25)	2.87(-25)	7.59(-26)
1.675	3.34(-25)	3.21(-25)	2.74(-25)	7.31(-26)

TABLE I (Continued)

Z = 13

T_o = 1.7 MeV

k (MeV)	dσ/dΩdk (cm^2/sr-MeV)		
θ =	30°	40°	60°
0.156	2.42(-24)	1.04(-24)	2.96(-25)
0.186	1.74(-24)	7.53(-25)	2.09(-25)
0.216	1.50(-24)	6.39(-25)	1.71(-25)
0.245	1.25(-24)	5.24(-25)	1.38(-25)
0.275	1.08(-24)	4.57(-25)	1.21(-25)
0.305	9.38(-25)	3.85(-25)	1.01(-25)
0.335	8.20(-25)	3.44(-25)	8.96(-26)
0.364	7.12(-25)	3.00(-25)	7.45(-26)
0.394	6.44(-25)	2.59(-25)	6.46(-26)
0.424	5.56(-25)	2.25(-25)	5.58(-26)
0.454	5.16(-25)	2.07(-25)	5.11(-26)
0.484	4.47(-25)	1.73(-25)	4.70(-26)
0.513	4.11(-25)	1.63(-25)	3.89(-26)
0.543	3.85(-25)	1.43(-25)	3.52(-26)
0.573	3.36(-25)	1.29(-25)	2.99(-26)
0.603	3.07(-25)	1.22(-25)	2.88(-26)
0.633	2.87(-25)	9.98(-26)	2.61(-26)
0.662	2.53(-25)	9.39(-26)	2.25(-26)
0.692	2.25(-25)	8.72(-26)	2.18(-26)
0.722	2.12(-25)	7.69(-26)	2.05(-26)
0.752	1.98(-25)	6.78(-26)	1.71(-26)
0.781	1.74(-25)	6.88(-26)	1.50(-26)
0.811	1.55(-25)	6.11(-26)	1.45(-26)
0.841	1.56(-25)	5.47(-26)	1.38(-26)
0.871	1.33(-25)	4.49(-26)	1.09(-26)
0.901	1.24(-25)	4.86(-26)	1.15(-26)
0.930	1.23(-25)	4.48(-26)	1.02(-26)
0.960	1.07(-25)	4.30(-26)	1.04(-26)
0.990	1.06(-25)	3.65(-26)	9.23(-27)
1.020	9.23(-26)	3.62(-26)	7.64(-27)
1.050	8.45(-26)	3.22(-26)	7.46(-27)
1.079	7.71(-26)	2.88(-26)	7.72(-27)
1.109	7.17(-26)	2.84(-26)	5.76(-27)
1.139	6.04(-26)	2.08(-26)	7.35(-27)
1.169	6.94(-26)	2.34(-26)	5.88(-27)
1.198	6.00(-26)	2.33(-26)	6.09(-27)
1.228	6.34(-26)	2.02(-26)	5.32(-27)
1.258	5.20(-26)	1.95(-26)	4.21(-27)
1.288	4.43(-26)	1.53(-26)	4.46(-27)
1.318	4.49(-26)	1.60(-26)	4.29(-27)
1.347	4.18(-26)	1.87(-26)	4.54(-27)
1.377	4.33(-26)	1.40(-26)	3.54(-27)
1.407	3.75(-26)	1.48(-26)	3.08(-27)
1.437	3.73(-26)	1.34(-26)	3.32(-27)
1.467	3.22(-26)	1.00(-26)	2.89(-27)
1.496	2.81(-26)	1.09(-26)	3.19(-27)
1.526	2.28(-26)	1.07(-26)	1.84(-27)
1.556	2.37(-26)	6.89(-27)	1.95(-27)
1.586	2.58(-26)	7.27(-27)	2.14(-27)
1.61,	1.67(-26)	7.03(-27)	1.80(-27)
1.645	1.91(-26)	7.52(-27)	1.83(-27)
1.675	1.41(-26)	5.29(-27)	1.48(-27)

TABLE I (Continued)

Z = 13

T_o = 2.5 MeV

k (MeV)	dσ/dΩdk (cm^2/sr-MeV)				
	θ = 0°	4°	10°	20°	30°
0.227	9.51(-23)	6.34(-23)	1.93(-23)	3.91(-24)	1.35(-24)
0.272	7.66(-23)	5.13(-23)	1.49(-23)	3.02(-24)	1.03(-24)
0.317	6.79(-23)	4.56(-23)	1.35(-23)	2.62(-24)	9.17(-25)
0.362	5.71(-23)	3.96(-23)	1.15(-23)	2.19(-24)	7.58(-25)
0.407	5.30(-23)	3.59(-23)	1.04(-23)	1.95(-24)	6.49(-25)
0.451	4.55(-23)	2.97(-23)	8.73(-24)	1.58(-24)	5.29(-25)
0.496	3.87(-23)	2.61(-23)	7.66(-24)	1.40(-24)	4.67(-25)
0.541	3.35(-23)	2.31(-23)	6.71(-24)	1.21(-24)	4.03(-25)
0.586	2.93(-23)	2.03(-23)	5.98(-24)	1.08(-24)	3.50(-25)
0.631	2.73(-23)	1.84(-23)	5.27(-24)	9.50(-25)	2.99(-25)
0.676	2.27)-23)	1.59(-23)	4.80(-24)	8.33(-25)	2.81(-25)
0.721	2.10(-23)	1.50(-23)	4.31(-24)	7.29(-25)	2.44(-25)
0.765	1.94(-23)	1.32(-23)	3.87(-24)	6.82(-25)	2.21(-25)
0.810	1.73(-23)	1.21(-23)	3.60(-24)	6.01(-25)	1.94(-25)
0.855	1.50(-23)	1.15(-23)	3.37(-24)	5.48(-25)	1.69(-25)
0.900	1.46(-23)	9.90(-24)	2.98(-24)	4.88(-25)	1.54(-25)
0.945	1.26(-23)	9.76(-24)	2.79(-24)	4.48(-25)	1.44(-25)
0.990	1.21(-23)	8.63(-24)	2.62(-24)	3.96(-25)	1.27(-25)
1.035	1.10(-23)	8.19(-24)	2.37(-24)	4.04(-25)	1.18(-25)
1.079	9.52(-24)	7.54(-24)	2.19(-24)	3.49(-25)	1.14(-25)
1.124	9.19(-24)	6.54(-24)	2.08(-24)	3.10(-25)	1.01(-25)
1.169	8.62(-24)	5.96(-24)	1.91(-24)	3.07(-25)	9.48(-26)
1.214	7.79(-24)	5.82(-24)	1.84(-24)	2.66(-25)	8.13(-26)
1.259	7.32(-24)	5.34(-24)	1.64(-24)	2.57(-25)	8.45(-26)
1.304	6.79(-24)	5.01(-24)	1.68(-24)	2.42(-25)	7.07(-26)
1.348	6.51(-24)	4.81(-24)	1.48(-24)	2.26(-25)	7.11(-26)
1.393	6.07(-24)	4.36(-24)	1.41(-24)	2.08(-25)	6.91(-26)
1.438	5.84(-24)	4.28(-24)	1.26(-24)	1.82(-25)	5.92(-26)
1.483	5.07(-24)	3.72(-24)	1.28(-24)	1.68(-25)	5.68(-26)
1.528	4.85(-24)	3.61(-24)	1.05(-24)	1.50(-25)	5.25(-26)
1.573	4.67(-24)	3.56(-24)	1.16(-24)	1.49(-25)	4.62(-26)
1.618	3.91(-24)	3.20(-24)	1.10(-24)	1.46(-25)	3.82(-26)
1.662	3.70(-24)	2.65(-24)	9.75(-25)	1.45(-25)	3.85(-26)
1.707	3.58(-24)	2.79(-24)	8.89(-25)	1.22(-25)	3.16(-26)
1.752	3.65(-24)	2.54(-24)	8.26(-25)	1.18(-25)	3.52(-26)
1.797	2.99(-24)	2.32(-24)	8.58(-25)	9.75(-26)	3.62(-26)
1.842	2.52(-24)	2.44(-24)	7.99(-25)	9.71(-26)	2.82(-26)
1.887	2.52(-24)	5.17(-24)	6.85(-25)	8.45(-26)	2.76(-26)
1.932	2.36(-24)	1.91(-24)	6.49(-25)	8.94(-26)	2.57(-26)
1.976	1.94(-24)	1.78(-24)	5.79(-25)	6.12(-26)	2.34(-26)
2.021	2.05(-24)	1.98(-24)	5.92(-25)	7.48(-26)	2.43(-26)
2.066	1.79(-24)	1.78(-24)	5.57(-25)	7.67(-26)	2.05(-26)
2.111	1.91(-24)	1.43(-24)	4.92(-25)	7.20(-26)	1.78(-26)
2.156	1.50(-24)	1.39(-24)	5.08(-25)	7.20(-26)	1.81(-26)
2.201	1.28(-24)	1.36(-24)	4.62(-25)	6.17(-26)	1.92(-26)
2.245	9.97(-25)	1.36(-24)	4.25(-25)	6.35(-26)	2.02(-26)
2.290	8.62(-25)	9.94(-25)	3.05(-25)	4.44(-26)	1.66(-26)
2.335	8.58(-25)	1.04(-24)	3.46(-25)	4.78(-26)	1.25(-26)
2.380	8.50(-25)	8.45(-25)	3.24(-25)	4.67(-26)	1.35(-26)
2.425	4.79(-25)	7.28(-25)	3.00(-25)	4.38(-26)	1.49(-26)
2.470	2.84(-25)	7.49(-25)	2.93(-25)	4.64(-26)	1.22(-26)

TABLE II

EXPERIMENTAL ELECTRON-BREMSSTRAHLUNG CROSS SECTIONS OBTAINED WITH Pb BEAM HARDENER

Note: The values used in this table are to be used in preference to the corresponding values in Table I because of their improved statistical accuracy.

Z = 13

T_o = 1.0 MeV

k (MeV)	$d\sigma/d\Omega dk$ (cm^2/sr-MeV)				
	θ = 0°	10°	20°	30°	40°
0.607	2.57(-24)	1.90(-24)		3.06(-25)	1.10(-25)
0.624	2.45(-24)	1.85(-24)		2.78(-25)	1.27(-25)
0.641	2.20(-24)	1.78(-24)		2.59(-25)	1.02(-25)
0.659	1.99(-24)	1.54(-24)		2.48(-25)	1.02(-25)
0.676	1.91(-24)	1.47(-24)		2.18(-25)	8.80(-26)
0.693	1.72(-24)	1.31(-24)	5.88(-25)	2.15(-25)	7.65(-26)
0.710	1.53(-24)	1.27(-24)	5.45(-25)	2.03(-25)	7.47(-26)
0.727	1.31(-24)	1.13(-24)	5.03(-25)	1.87(-25)	6.69(-26)
0.744	1.37(-24)	1.00(-24)	4.68(-25)	1.58(-25)	6.17(-26)
0.761	1.13(-24)	1.00(-24)	4.46(-25)	1.53(-25)	5.49(-26)
0.778	9.64(-25)	9.25(-25)	4.10(-25)	1.46(-25)	5.74(-26)
0.795	9.62(-25)	8.23(-25)	3.77(-25)	1.26(-25)	4.42(-26)
0.812	8.30(-25)	7.81(-25)	3.68(-25)	1.24(-25)	4.42(-26)
0.829	7.87(-25)	7.48(-25)	3.31(-25)	1.12(-25)	4.18(-26)
0.846	5.48(-25)	6.62(-25)	3.08(-25)	1.13(-25)	4.09(-26)
0.863	5.34(-25)	5.89(-25)	2.88(-25)	1.03(-25)	4.33(-26)
0.880	4.27(-25)	5.12(-25)	2.61(-25)	1.01(-25)	3.91(-26)
0.897	3.42(-25)	4.70(-25)	2.41(-25)	9.01(-26)	3.87(-26)
0.914	2.76(-25)	4.23(-25)	2.24(-25)	8.45(-26)	3.07(-26)
0.931	2.60(-25)	3.91(-25)	2.13(-25)	6.74(-26)	2.79(-26)
0.948	2.42(-25)	3.81(-25)	1.78(-25)	7.35(-26)	2.91(-26)
0.965	1.68(-25)	2.87(-25)	1.66(-25)	5.91(-26)	2.53(-26)
0.982	1.08(-25)	2.48(-25)	1.68(-25)	5.13(-26)	1.79(-26)
0.999	9.53(-26)	2.07(-25)	1.51(-25)	4.05(-26)	1.92(-26)

TABLE II (Continued)

Z = 29

T_0 = 1.0 MeV

k (MeV)	$d\sigma/d\Omega dk$ (cm^2/sr-MeV)				
	θ = 0°	10°	20°	30°	40°
0.522	2.05(-23)		6.11(-24)		
0.539	2.00(-23)		6.09(-24)		
0.556	1.88(-23)		6.02(-24)		
0.573	1.76(-23)		5.63(-24)		
0.590	1.60(-23)		5.22(-24)		
0.607	1.56(-23)	1.11(-23)	5.02(-24)	1.86(-24)	7.73(-25)
0.624	1.35(-23)	1.07(-23)	4.80(-24)	1.75(-24)	7.08(-25)
0.641	1.29(-23)	9.96(-24)	4.43(-24)	1.57(-24)	6.58(-25)
0.659	1.18(-23)	9.32(-24)	4.27(-24)	1.59(-24)	6.29(-25)
0.676	1.12(-23)	8.62(-24)	3.94(-24)	1.48(-24)	5.98(-25)
0.693	1.00(-23)	8.30(-24)	3.71(-24)	1.32(-24)	5.24(-25)
0.710	9.19(-24)	7.43(-24)	3.49(-24)	1.27(-24)	4.94(-25)
0.727	8.49(-24)	7.09(-24)	3.07(-24)	1.23(-24)	4.47(-25)
0.744	8.14(-24)	6.34(-24)	3.08(-24)	1.12(-24)	4.14(-25)
0.761	7.10(-24)	6.10(-24)	2.72(-24)	1.02(-24)	3.94(-25)
0.778	6.59(-24)	5.53(-24)	2.69(-24)	1.00(-24)	3.85(-25)
0.795	5.94(-24)	5.44(-24)	2.48(-24)	9.31(-25)	3.63(-25)
0.812	4.96(-24)	4.87(-24)	2.29(-24)	8.67(-25)	3.10(-25)
0.829	4.62(-24)	4.68(-24)	2.22(-24)	7.71(-25)	2.99(-25)
0.846	4.36(-24)	3.99(-24)	2.08(-24)	7.11(-25)	2.95(-25)
0.863	3.61(-24)	3.66(-24)	1.78(-24)	6.97(-25)	2.62(-25)
0.880	3.34(-24)	3.54(-24)	1.80(-24)	6.61(-25)	2.32(-25)
0.897	2.89(-24)	3.20(-24)	1.71(-24)	6.27(-25)	2.47(-25)
0.914	2.63(-24)	2.79(-24)	1.60(-24)	5.39(-25)	2.47(-25)
0.931	1.97(-24)	2.66(-24)	1.48(-24)	5.49(-25)	2.09(-25)
0.948	1.71(-24)	2.49(-24)	1.31(-24)	5.08(-25)	2.08(-25)
0.965	1.57(-24)	2.31(-24)	1.37(-24)	5.07(-25)	1.80(-25)
0.982	1.32(-24)	2.25(-24)	1.26(-24)	4.99(-25)	1.88(-25)
0.999	8.45(-25)	1.85(-24)	1.15(-24)	4.01(-25)	1.69(-25)

TABLE II (Continued)

Z = 50

T_o = 1.0 MeV

k (MeV)	dσ/dΩdk (cm^2/sr-MeV)	
	θ = 40°	60°
0.522	2.95(-24)	8.06(-25)
0.539	2.90(-24)	8.44(-25)
0.556	2.66(-24)	7.46(-25)
0.573	2.67(-24)	6.96(-25)
0.590	2.32(-24)	6.58(-25)
0.607	2.23(-24)	5.78(-25)
0.624	2.13(-24)	5.78(-25)
0.641	1.98(-24)	5.23(-25)
0.659	1.84(-24)	4.81(-25)
0.676	1.82(-24)	4.92(-25)
0.693	1.73(-24)	4.43(-25)
0.710	1.59(-24)	4.05(-25)
0.727	1.47(-24)	3.79(-25)
0.744	1.32(-24)	3.09(-25)
0.761	1.34(-24)	3.45(-25)
0.778	1.16(-24)	2.62(-25)
0.795	1.16(-24)	2.95(-25)
0.812	1.09(-24)	2.57(-25)
0.829	1.05(-24)	2.52(-25)
0.846	9.53(-25)	2.58(-25)
0.863	9.09(-25)	2.27(-25)
0.880	8.04(-25)	2.18(-25)
0.897	8.10(-25)	1.81(-25)
0.914	7.43(-25)	1.80(-25)
0.931	7.74(-25)	1.67(-25)
0.948	6.92(-25)	1.75(-25)
0.965	6.79(-25)	1.50(-25)
0.982	6.91(-25)	1.80(-25)
9.999	6.51(-25)	1.40(-25)

Z = 79

T_o = 1.0 MeV

k (MeV)	dσ/dΩdk (cm^2/sr-MeV)
	θ = 40°
0.522	9.70(-24)
0.539	9.86(-24)
0.556	9.41(-24)
0.573	8.79(-24)
0.590	8.47(-24)
0.607	8.11(-24)
0.624	7.60(-24)
0.641	7.22(-24)
0.659	6.79(-24)
0.676	6.40(-24)
0.693	6.10(-24)
0.710	5.73(-24)
0.727	5.57(-24)
0.744	4.94(-24)
0.761	4.88(-24)
0.778	4.81(-24)
0.795	4.38(-24)
0.812	4.09(-24)
0.829	3.82(-24)
0.846	3.59(-24)
0.863	3.48(-24)
0.880	3.55(-24)
0.897	3.19(-24)
0.914	2.94(-24)
0.931	3.03(-24)
0.948	2.73(-24)
0.965	2.66(-24)
0.982	2.52(-24)
0.999	2.49(-24)

TABLE II (Continued)

Z = 13

T_o = 1.7 MeV

k (MeV)	dσ/dΩdk (cm^2/sr-MeV)			
	θ = 0°	4°	10°	
1.198	2.36(-24)	1.92(-24)	9.89(-25)	
1.228	2.09(-24)	1.83(-24)	9.12(-25)	
1.258	2.04(-24)	1.69(-24)	8.98(-25)	
1.288	1.83(-24)	1.52(-24)	8.32(-25)	
1.318	1.76(-24)	1.45(-24)	7.65(-25)	
1.347	1.62(-24)	1.27(-24)	7.14(-25)	
1.377	1.39(-24)	1.25(-24)	6.99(-25)	
1.407	1.23(-24)	1.08(-24)	6.62(-25)	
1.437	1.19(-24)	1.00(-24)	5.51(-25)	
1.467	1.05(-24)	8.62(-25)	5.20(-25)	
1.496	8.65(-25)	8.29(-25)	4.72(-25)	
1.526	7.50(-25)	7.07(-25)	4.48(-25)	
1.556	6.14(-25)	6.50(-25)	4.28(-25)	
1.586	5.95(-25)	5.60(-25)	3.54(-25)	
1.615	3.82(-25)	4.76(-25)	3.62(-25)	
1.645	3.43(-25)	4.01(-25)	2.67(-25)	
1.675	2.86(-25)	3.36(-25)	2.34(-25)	

	θ = 20°	30°	40°	60°
0.901	4.06(-25)	1.22(-25)	4.65(-26)	1.09(-26)
0.930	4.08(-25)	1.22(-25)	4.46(-26)	1.07(-26)
0.960	3.89(-25)	1.05(-25)	4.04(-26)	1.00(-26)
0.990	3.58(-25)	1.04(-25)	3.78(-26)	9.60(-27)
1.020	3.59(-25)	1.00(-25)	3.78(-26)	8.85(-27)
1.050	3.04(-25)	8.98(-26)	3.24(-26)	8.15(-27)
1.079	2.99(-25)	8.06(-26)	2.93(-26)	7.31(-27)
1.109	2.62(-25)	7.87(-26)	2.82(-26)	6.69(-27)
1.139	2.60(-25)	7.05(-26)	2.52(-26)	6.45(-27)
1.169	2.36(-25)	6.44(-26)	2.54(-26)	5.98(-27)
1.198	2.24(-25)	5.96(-26)	2.51(-26)	5.49(-27)
1.228	2.15(-25)	5.98(-26)	2.37(-26)	5.08(-27)
1.258	2.05(-25)	6.00(-26)	2.11(-26)	4.76(-27)
1.288	1.84(-25)	4.72(-26)	2.13(-26)	4.21(-27)
1.318	1.57(-25)	4.86(-26)	1.67(-26)	4.12(-27)
1.347	1.65(-25)	4.69(-26)	1.73(-26)	3.93(-27)
1.377	1.52(-25)	4.24(-26)	1.65(-26)	3.12(-27)
1.407	1.41(-25)	3.83(-26)	1.47(-26)	3.94(-27)
1.437	1.32(-25)	3.69(-26)	1.35(-26)	3.27(-27)
1.467	1.22(-25)	3.41(-26)	1.43(-26)	3.52(-27)
1.496	1.13(-25)	3.30(-26)	1.17(-26)	2.95(-27)
1.526	1.04(-25)	3.08(-26)	1.16(-26)	2.72(-27)
1.556	9.72(-26)	3.28(-26)	9.66(-27)	2.21(-27)
1.586	9.66(-26)	2.41(-26)	1.04(-26)	2.38(-27)
1.615	8.67(-26)	2.53(-26)	8.13(-27)	2.13(-27)
1.645	7.91(-26)	1.69(-26)	6.98(-27)	1.54(-27)
1.675	5.58(-26)	1.70(-26)	6.58(-27)	1.63(-27)

TABLE II (Continued)

Z = 13

T_o = 2.5 MeV

k (MeV)	$d\sigma/d\Omega dk$ (cm^2/sr-MeV)				
	θ = 0°	4°	10°	20°	30°
1.348	5.54(-24)	4.29(-24)	1.28(-24)	2.18(-25)	5.08(-26)
1.393	5.70(-24)	4.35(-24)	1.27(-24)	2.16(-25)	4.87(-26)
1.438	5.37(-24)	4.06(-24)	1.19(-24)	2.04(-25)	5.05(-26)
1.483	5.14(-24)	3.73(-24	1.13(-24)	1.97(-25)	4.32(-26)
1.528	4.52(-24)	3.51(-24)	1.10(-24)	1.87(-25)	3.98(-26)
1.573	4.18(-24)	3.22(-24)	1.03(-24)	1.65(-25)	3.67(-26)
1.618	4.06(-24)	3.24(-24)	1.01(-24)	1.61(-25)	3.21(-26)
1.662	3.89(-24)	2.89(-24)	9.39(-25)	1.48(-25)	3.50(-26)
1.707	3.40(-24)	2.83(-24)	8.50(-25)	1.34(-25)	3.01(-26)
1.752	3.30(-24)	2.66(-24)	8.07(-25)	1.30(-25)	2.81(-26)
1.797	2.99(-24)	2.48(-24)	7.52(-25)	1.23(-25)	2.62(-26)
1.842	2.69(-24)	2.17(-24)	7.23(-25)	1.10(-25)	2.62(-26)
1.887	2.48(-24)	2.15(-24)	6.72(-25)	1.02(-25)	2.32(-26)
1.932	2.36(-24)	2.02(-24)	6.23(-25)	9.83(-26)	2.17(-26)
1.976	2.17(-24)	1.86(-24)	5.86(-25)	9.32(-26)	2.58(-26)
2.021	1.95(-24)	1.76(-24)	5.45(-25)	8.53(-26)	1.94(-26)
2.066	1.82(-24)	1.46(-24)	5.31(-25)	8.30(-26)	1.69(-26)
2.111	1.54(-24)	1.45(-24)	4.64(-25)	7.09(-26)	1.93(-26)
2.156	1.51(-24)	1.30(-24)	4.07(-25)	7.06(-26)	1.68(-26)
2.201	1.24(-24)	1.23(-24)	3.78(-25)	6.56(-26)	1.45(-26)
2.245	1.24(-24)	1.14(-24)	3.54(-25)	6.43(-26)	1.55(-26)
2.290	9.53(-25)	1.05(-24)	3.31(-25)	5.86(-26)	1.52(-26)
2.335	9.68(-25)	8.43(-25)	3.07(-25)	5.93(-26)	1.24(-26)
2.380	6.52(-25)	8.11(-25)	2.87(-25)	4.88(-26)	1.15(-26)
2.425	4.47(-25)	6.77(-25)	2.66(-25)	4.94(-26)	1.26(-26)
2.470	3.56(-25)	7.18(-25)	2.67(-25)	5.36(-26)	1.16(-26)

NASA-Langley, 1967 —— 24 CR-759